IEEE Access
Multidisciplinary | Rapid Review | Open Access Journal

Received 8 December 2023, accepted 16 January 2024, date of publication 19 January 2024, date of current version 29 January 2024.

Digital Object Identifier 10.1109/ACCESS.2024.3356173

RESEARCH ARTICLE

Compressible Non-Newtonian Fluid Based Road Traffic Flow Equation Solved by Physical-Informed Rational Neural Network

ZAN YANG[1], DAN LI[1], WEI NAI[2,3], (Member, IEEE), LU LIU[4], JINGJING SUN[2,3], AND XIAOWEI LV[2,3]

[1]Public Teaching and Research Department, Huzhou College, Huzhou 313000, China
[2]School of Electronic Information, Huzhou College, Huzhou 313000, China
[3]Huzhou Key Laboratory for Urban Multidimensional Perception and Intelligent Computing, Huzhou College, Huzhou 313000, China
[4]School of Business, St. Bonaventure University, St. Bonaventure, NY 14778, USA

Corresponding author: Wei Nai (niwei@zjhzu.edu.cn)

This work was supported in part by the General Scientific Research Fund of Zhejiang Provincial Education Department under Grant Y202351125; in part by the Huzhou Natural Science Fund Project under Grant 2023YZ35; and in part by the Initial Scientific Research Fund of Talent Introduction in Huzhou College under Grant RK59004, Grant RK59006, and Grant RK64001.

ABSTRACT The study of road traffic flow theory utilizes physics and applied mathematics to analyze relevant parameters and their relationships quanlitatively and quantitatively, in order to explore their dynamic changes. The fluid dynamics model used for traffic flow analysis is highly favored by scholars due to its solid mathematical foundation and good simulation results. However, existing models have two main shortcomings: firstly, existing research is mostly limited to non-viscoelastic fluid equation or incompressible non-Newtonian fluid equation, making it difficult to accurately describe the viscosity state and micro cluster properties of the actual traffic flow; secondly, the existing non-Newtonian fluid partial differential equations (PDEs) rely heavily on the finite element method (FEM) for solving, requiring higher computational cost, larger storage space, and more constraint conditions. Thus, in this paper, a traffic flow equation based on compressible non-Newtonian fluid has been constructed, and it has been solved by using physical-informed rational neural network (PIRNN) and noise heavy-ball acceleration gradient descent (NHAGD) to ensure learning and training speed and accuracy. Numerical results indicate that the proposed method can truly reflect the gradual change process in the viscosity of traffic flow, and has better solving performance than traditional FEM and physical-informed neural network (PINN) with activation functions; under the same conditions, the prediction error of the proposed method is also smaller than that of traditional traffic flow models.

INDEX TERMS Traffic flow analysis, compressible non-Newtonian fluid, partial differential equation (PDE) solution, physical-informed rational neural network (PIRNN), activation function.

I. INTRODUCTION

Data has shown that China's urbanization process has been continuously accelerating, at the end of the year 2021, the urbanization rate of China's resident population has reached up to 64.72% [1]. In the expanding scale of large and medium-sized cities, limited urban transportation resources and increasing transportation demand have formed a significant supply-demand contradiction [2]. It is very important to achieve effective governance of urban transportation and solve congestion problems as much as possible, and such effective governance relies on a deep understanding of the rules of urban transportation travel. The theoretical research of road traffic flow is to use physics and applied mathematics

The associate editor coordinating the review of this manuscript and approving it for publication was Mounim A. El Yacoubi.

to conduct qualitative and quantitative research on its parameters and their interrelationships in order to seek its dynamic change law (theoretical validity). Among many traffic flow theories, fluid dynamics models have attracted the attention of scholars in the field of transportation engineering due to their solid mathematical foundation and good simulation results [3], [4], [5]. Therefore, based on fluid dynamics models, it is of great significance to get higher accuracy in interpreting the changes in actual road traffic flow, assisting urban traffic managers in understanding the changes in road flow, making more reasonable control decisions, and improving the mobility of urban road traffic systems.

In recent years, although the methodology based on fluid dynamics, especially the non-Newtonian fluid partial differential equation (PDE) solution, has been favored by more and more scholars in explaining the fluid motion laws with complex characteristics, however, non-Newtonian fluid PDE still has two defects in explaining the traffic flow problems: firstly, the existing research is mostly limited to the traffic flow equations based on the non viscoelastic fluid equations or incompressible non-Newtonian fluid, and cannot accurately describe the viscosity state and micro cluster properties of actual traffic flow; secondly, most of the existing non-Newtonian fluid PDEs are solved based on finite element method (FEM), which requires higher computational costs, larger storage space, and more constraints. In recent years, physical-informed neural network (PINN) has shown its advantages in the field of numerical calculation of PDEs, but its neural network (NN) based on the traditional activation function still does not reach the optimal approximation degree of physical rules. The above defects constitute the research motivation of this paper, to be specific, a novel compressible non-Newtonian fluid based road traffic flow equation has been proposed in this paper, its learning and training speed can be ensured by solving it through physical information rational neural network (PIRNN) and noise heavy-ball acceleration gradient descent (NHAGD) methods. Numerical results show that the proposed method can faithfully reflect the gradual change process in the viscosity of traffic flow, and has better performance than traditional FEM and PINN with activation function in solving PDEs.

The rest of this paper will be organized as follows: in Section II, the related theoretical research involved in the traffic flow analysis will be reviewed, especially the application of non-Newtonian fluid theory in the field including but not limited to traffic flow analysis, and the research application of the corresponding PDE solution; in Section III, the basic traffic flow model and its physical assumptions based on compressible non-Newtonian fluid established in this paper will be described; in Section IV, the solution of the established compressible non-Newtonian fluid based traffic flow PDE will be discussed; in Section V, the model proposed in this paper will be applied to a two-way single lane road in Huzhou City to verify its effectiveness in explaining the objective laws of urban road traffic flow; while in Section VI, the research content of this paper will be summarized, and some ideas for future research will also be proposed.

II. LITERATURE REVIEW

A. EMERGING THEORY OF TRAFFIC FLOW

In the past few years, many scholars in the field of transportation have refined the traditional general traffic flow theory under different scene conditions as their research direction. At the same time, the emergence of various emerging algorithms, including artificial intelligence (AI), has also given new vitality to traditional traffic flow theory.

For the study of traffic flow changes in different scenarios, Zhang et al. have used the travel time index (TTI) probability distribution model to give a universally description of the traffic flow dispersion phenomenon under different road lengths and average speed conditions [6]; Wang et al. have considered a dynamic traffic flow model with intersections as constraints and defined an optimization objective function based on parameters such as intersection throughput and driver waiting time, in order to establish a real-time adaptive traffic control system [7]; Yan et al. have also designed a time-varying multi-parameter iterative learning identification strategy for the constraints on traffic flow at intersections, making the established refined traffic flow model approach the true description of the number of vehicles queuing at intersections [8]; Dabiri et al. have proposed to parameterize and modify traditional traffic flow models by categorizing the severity of specific events in response to abnormal situations in traffic flow [9]; Ni et al. have analyzed the impact of rainfall on the distribution of traffic flow after waterlogging, and have particularly discussed the increase in traffic flow density caused by insufficient downstream road capacity in waterlogged areas [10]; Zhang et al. have constructed equations that consider the conservation of mass and acceleration in each lane for traffic flow in a dual lane and dual speed scenario, and have established their accurate Riemannian solutions [11].

Some scholars have also conducted research on the calibration and validation of traditional traffic flow models in new scenarios. Jin et al. have calibrated traffic flow motion models in discrete space and time under different driving strategies and potential trends based on cellular automata (CA) theory [12]; Poole et al. have compared the traffic flow models integrating different algorithms based on gradient and particle swarm optimization (PSO) to explain the macro traffic flow of large expressway networks, and have pointed out that the combined algorithm can achieve better results [13]; Similarly, Wang et al. have calibrated and validated some of the traffic flow models, taking into account factors such as congestion, flow non-uniformity, stopping waves, adverse weather, and accidents, and have pointed out that they can meet the interpretation needs of complex traffic flow dynamics in large high-speed networks [14]. Li et al. have discussed the individual heterogeneity of traffic flow formation, by taking different driving styles of aggressiveness, they improved the traditional mixed traffic flow theory [15]; likewise, Tian et al.

have discussed the impact of different degrees of automated vehicle (AV) or connected automated vehicle (CAV) permeability on traffic flow [16].

In terms of the integration of AI algorithm and traditional traffic flow theory, Mo et al. have analyzed the content of Microblog APP published by urban traffic police based on the fuzzy comprehensive language evaluation algorithm, to determine the dynamic evolution of urban traffic flow in terms of congestion time and location [17]; Wang et al. have used the k-means clustering algorithm to cluster roads with the same traffic flow feature type, and have trained a backpropagation NN based on PSO to achieve more accurate anomaly detection of road traffic conditions [18]; Ai et al. have used branch analysis to improve the classic macro traffic theory, and have achieved a more accurate description of nonlinear phenomena such as frequent starting and stopping on urban roads, as well as local aggregation [19]; Storm et al. have established Gaussian process approximation for stochastic traffic flow models, and have achieved accurate expression of vehicle density in any topological road traffic network [20]; Yuan et al. have introduced machine learning (ML) algorithm into traditional traffic flow models, encoding traffic flow as a multivariate Gaussian process, and implementing the encoding of complex traffic flow model increments in the ML algorithm, making the traffic flow model lightweight and with higher computational efficiency [21]. Zeng et al. have tried to propose a lane level traffic flow model based on the deep learning (DL) framework, and have tried to mine the spatial correlation of traffic flow on the time complex network based on the visibility map [22].

B. APPLICATIONS OF NON-NEWTONIAN FLUID THEORY

Non-Newtonian fluid, as a type of fluid that can describe viscoelastic characteristics, have unique advantages in reflecting velocity fields that do not strictly possess traditional fluid properties, and have received widespread attention from scholars in recent years [23], [24]. In the field of life and health, Redfearn et al. have applied non-Newtonian fluid to explain the rheology behavior of different food in mouth, and have discussed the compression characteristics of tongue and upper jaw on food fluids during eating [25]; Shi et al. have used non-Newtonian fluid theory to simulate the physical characteristics of bleeding, incorporating the effects of tension and platelets on the viscosity of bleeding particles into the non-Newtonian fluid equation, making the theoretical description closer to the true biological characteristics of bleeding [26]; Bhatti et al. have studied the motion of metal suspended substances in nanofluids and explained the delivery law of magnetic drugs in narrow arteries using non-Newtonian fluid theory [27].

In the past five years, non-Newtonian fluid has been widely used as a tool for analyzing traffic flow with viscoelasticity, which is undoubtedly a revolutionary change compared to traditional traffic flow theory. Zhang et al. and Ma et al. have both pointed out that traffic flow has properties similar to non-Newtonian fluid, by using the time distance of spatial vehicle heads to characterize traffic pressure, they have attempted to investigate the impact of maximum relaxation of the model on circular roads and the rationality of non-Newtonian fluid in describing traffic flow [28], [29]; Sun et al. have constructed a basic model of macroscopic traffic flow using equations derived from non-Newtonian fluid, and have particularly pointed out that the viscosity in traffic flow is related to the delay time of vehicle movement and the speed of motion waves during congestion [30]; Kang et al. have emphasized the non-negligible nature of viscoelasticity in traffic flow and have pointed out the rationality of using non-Newtonian fluid to explain traffic flow [31]; Karafylis et al. have introduced pressure and viscosity terms specifically for the 2-dimensional motion of bicycle traffic flow in the absence of lanes, attempting to quantify the impact of adjacent vehicles and road boundaries on traffic flow through a new fluid expression with non-Newtonian fluid properties, and applying it in the design of autonomous cruise controllers [32].

C. SOLVING PDES BASED ON FEM

The description of non-Newtonian fluid involves PDEs, and the search for the law of non-Newtonian fluid must involve the solution of PDEs. In fact, although some studies on traffic flow do not involve non-Newtonian fluid models, PDEs are also used in the description of traffic flow [33], [34].

Currently, the effective solution of PDEs has been a long-term open challenge. Except for a few differential equations that can directly obtain analytical solutions, more equations can only rely on numerical methods for approximate solutions, such as FEM. These methods usually divide the continuous problem domain into discrete grids, and then combine variational methods with piecewise interpolation methods for approximate calculations. Traditional numerical methods have shown some effectiveness in solving PDEs, but as the number of iterations increases, the computational efficiency also decreases significantly.

In terms of solving PDEs, Stevenson et al. have attempted to use the finite element method to analyze parabolic PDE [35], while Metzger have used FEM to solve 4th-order PDE, so as to solve the liquid crystal flow characteristics in liquid crystal flow guides [36]. In describing the solution of PDE of non-Newtonian fluid, Memon et al. have used FEM simulate the heat transfer effect of non-Newtonian power law fluid on the surface of the end of a cylinder channel containing a mesh screen, and have pointed out that the heat transfer increases with the power exponent of non-Newtonian fluid [37]; Bilal et al. and Nawaz et al. have also studied the heat transfer characteristics of non-Newtonian fluid, and have used FEM to quantitatively solve the heat transfer characteristics of viscous fluid in different spaces and material environments [38], [39]; Hou et al. and Kune et al. have discussed the properties of non-Newtonian fluid under the influence of Soret and Dufour effects, and have solved the heat and mass transfer characteristics of fluids with different properties under chemical reaction using FEM [40], [41];

Omri et al. have used the generalized FEM to discretize PDE so as to solve the convection heat transfer effect of non-Newtonian mixed nano fluid in the 3-layer square cavity, and have reasonably approximated the temperature, speed and pressure of the fluid [42].

D. SOLVING PDES BASED ON PINN

As mentioned in Section II-C, the existing methods for solving PDEs based on FEM require grid partitioning and solving nonlinear equations, which results in high computational costs and difficult technological breakthroughs. Actually, In addition to FEM, Frey et al. and Sacchetti et al. have also discussed the feasibility of using NN to solve PDE, and attempted to use NN to solve PDEs with different boundary conditions and types. Their conclusions indicate that using NN to solve PDEs can achieve more accurate results than FEM, especially when it comes to analyze data with time properties or high-dimensional data, but the network structure of NN is often relatively complex [43], [44].

It also should be pointed out that for a long time, people have been hoping to find new numerical methods for PDEs that do not require grid partitioning or nonlinear equation solving. In recent years, PINN has led to significant changes in numerical simulation technology, and the method for solving PDEs based on PINN not only enables fast forward modeling and inversion modeling [45], [46], but also effectively solves nonlinear problems [47], [48], [49], and can solve more complex and high-dimensional PDEs [50], [51], [52]. Falini et al. and Zhi et al. have even argued that as PINN has better stability, it can be used as an alternative to the traditional FEM in solving PDEs [53], [54].

To be more specific, Pang et al. have proposed the fractional PINN (fPINN) method for solving fractional order PDEs [55], Lu et al. from the same research team have also provided the DeepXDE ML library for solving PDEs based on the PINN method, and this ML library for scientific computing has been widely used by many scholars in recent years [56]. Kharazmi et al. have proposed the variational PINN (VPINN) method, which for the first time combines the variational method with PINN [57], and subsequently, Kharazmi et al. have also combined domain decomposition technology with VPINN [58]. Yang et al. have combined Bayesian theory with PINN to propose BPINN for solving inverse problems of PDEs with noisy data [59]. Sun et al. have even proposed a second-order PINN combining with self-adaptive activation function policy and gradient enhancement policy to improve the performance of PINN in solving PDEs [60].

Just in the past few months, scholars have extensively attempted to use PINN to solve PDE in their own industry field. Roh et al. have attempted to use PINN to solve PDE in salinity transfer kinetics, and have demonstrated that this method has lower absolute deviation than ordinary artificial neural network (ANN) [61]; Singh et al. have integrated particle models into the training process of NN, and have used PINN to predict the charging state and health state of lithium-ion batteries for PDE [62]; Zhou et al. have even combined PINN with traditional FEM and have proposed an integrated smooth finite element method (SFEM) to solve elastic-plastic forward and inverse PDEs, which have achieved lower error [63].

However, it can be seen that till now, PINN has very few applications in the field of transportation. In the current stage, there is only some progress in identifying traffic density [64], vehicle following models [65], estimating traffic states [66], [67], [68], and solving incompressible traffic flow fluid equations [69].

III. TRAFFIC FLOW MODELING BASED ON COMPRESSIBLE NON-NEWTONIAN FLUID DYNAMICS

A. BASIC IDEA OF THE MODEL

In fact, when establishing classical fluid dynamics equations, whether from a molecular perspective or a micro cluster perspective, there are always gaps between each unit and they are discrete. However, fluid flows over time, and its trajectory is continuous. In classical theory, density and speed are generally assumed to vary continuously depending on time and position coordinates, both of which are continuous variables. The classical fluid dynamics equations are established by assuming continuous changes in density and speed. And there have been articles describing traffic flow using continuous models for a long time, mainly focusing on the use of fluid dynamics models to explain traffic flow phenomena. For example, early and classic models such as the one proposed by Lighthill et al. [70], Pipes [71], Payne [72], Whitham [73], Phillips [74], Wu [75], Hoogendoorn et al. [76], and Helbing et al. [77], etc. Recently, there has been widespread attention to the hyperbolic traffic flow model proposed in literature [69] based on incompressible Newtonian flow theory to describe traffic fluids and the virtual fluid-flow-model (VFFM) proposed in literature [78]. However, there is no precedent for using compressible non-Newtonian flow models to describe traffic flow. In addition, all methods that rely on NNs to solve partial differential equations utilize discrete data during training, which essentially utilizes the universal approximation principle of NNs, which means that through a certain number of neurons, the potential continuous laws of discrete training data can be fitted. The essence of traffic flow modeling method based on compressible non-Newtonian fluid dynamics, is to add physical rule constraints during the fitting process, which balances data-driven and rule-driven approaches, so as to make the fitting effect more in line with physical rules and improve the scientific and interpretable nature of the method itself.

In Physics, fluids in fluid mechanics are composed of molecules which have gaps between themselves. From a microscopic point of view, fluids are not continuously distributed substances. However, for most engineering application problems, fluid mechanics does not study the motion of microscopic molecules, but rather the macroscopic motion

of fluids. In this context, the smallest fluid element can be recognized as fluid micro clusters with infinitesimal volumes. Thus, it is possible to ignore the gaps between molecules and not to discuss the motion of each molecule, but to recognize the fluid as a continuous medium composed of countless continuously distributed fluid micro clusters.

Likewise, traffic flow is composed of vehicles, and there are always certain distances between them. Also from a microscopic point of view, traffic flow is not continuously distributed. However, if several vehicles and the distances between them are referred to as a vehicle domain as first proposed by Xu et al., then traffic flow can be considered to be composed of vehicle domains, and thus can be regarded as a continuous flow with continuous distribution. Vehicle domains can be considered to fill the entire road and are compressible [79].

As mentioned in Section I, most of the existing traffic flow PDE models are based on incompressible non-Newtonian fluid dynamic equation. Such methods assume that the discrete elements in incompressible non-Newtonian fluid are molecules, which are equivalent to vehicles in the traffic flow system. This assumption is less rigorous and distorted compared to real traffic flow. The real traffic flow is often presented in the form of vehicle domain, and the vehicle domain is compressible both laterally and longitudinally, and it often has the viscous characteristics of non-Newtonian fluid when the traffic flow is congested or unblocked. Therefore, different from the existing literature, in this paper, the discrete element of compressible non-Newtonian fluid is assumed as a micro cluster, which is equivalent to the vehicle domain in the traffic flow system. In this way, a new traffic flow PDE model is given by using the non-Newtonian fluid dynamic equation for reference. Table 1 shows the conceptual equivalence relation between non-Newtonian fluid dynamics system and traffic flow system.

TABLE 1. Conceptual equivalence relation between non-Newtonian fluid dynamics system and traffic flow system.

Physical Characteristics	Non-Newtonian Fluid Dynamic System	Traffic Flow System
Continuum	Unidirectional compressible non-Newtonian fluid	Single lane traffic flow
Discrete Element	Micro Cluster	Vehicle domain
Variables	Density	Traffic flow density
	Speed	Traffic flow speed
	Pressure	Traffic pressure (from the flow)

To establish a compressible non-Newtonian traffic flow PDE, the following physical assumptions should be given in this paper: (1) The model scenario is set to single lane traffic flow. (2) Vehicle domain is equivalent to micro cluster in fluid dynamics, and the compressibility of vehicle domain is equivalent to the compressibility of micro cluster in fluid dynamics. (3) A 1-dimensional (1D) compressible non-Newtonian fluid PDE system for traffic flow is supposed to be established, so the vehicle domain can only be compressible laterally (coordinate in the flow direction). (4) The viscosity coefficient depends on density. This assumption is reasonable, because when the density increases, the traffic flow becomes denser, the traffic pressure increases, and the viscosity of vehicles increases, similar to the shear thickening flow in non-Newtonian fluid dynamics; while when the density decreases, the traffic flow becomes more sparse, the traffic pressure decreases, and the viscosity of vehicles decreases, similar to the shear thinning flow in non-Newtonian fluid dynamics.

Based on the consumptions above, the 1D compressible non-Newtonian traffic flow PDEs proposed in this paper can be written as follows:

$$\rho_t + (\rho u)_x = 0 \tag{1}$$

$$(\rho u)_t + (\rho u^2)_x - (\mu(\rho)u_x)_x + P_x = 0 \tag{2}$$

$$P \equiv P(\rho) = A_1\rho^{\gamma_1}, A_1 > 0,\ \gamma_1 > 1 \tag{3}$$

$$\mu \equiv \mu(\rho) = A_2\rho^{\gamma_2}, A_2 > 0,\ \gamma_2 > 1 \tag{4}$$

$$\rho(x,\ 0) = \rho_0 \geq 0, u(x,\ 0) = 0, \forall x \in (\kappa_1,\ \kappa_2) \tag{5}$$

$$u(\kappa_1,\ t) = u(\kappa_2,\ t) = 0, \forall t \in (0,\ T) \tag{6}$$

Equation (1) is the mass-conservation equation, mass-conservation refers to a closed system whose mass does not change with time and place, and always remains unchanged. Assuming the density and the speed of the traffic flow is $\rho(x, t)$ and $\boldsymbol{u}(x, t)$ respectively, and taking a segment of the traffic flow Ω as the object to study, Ω can be assumed as a smooth bounded open region. During the flowing process of the traffic flow, the change in fluid mass within Ω is

$$\int_\Omega \rho_t(x,\ t)\mathrm{d}x \tag{7}$$

Due to the mass-conservation principle, the amount of increase/decrease in mass within Ω must be equal to the net inflow/outflow of the area S enclosed by the boundary $\partial\Omega$ of Ω, which can be written as:

$$\int_{\partial\Omega} \rho\boldsymbol{u}\cdot\boldsymbol{n}\mathrm{d}S \tag{8}$$

where $\boldsymbol{n}$ is the unit outer normal vector of the area S, from (7) and (8), there is

$$\int_\Omega \rho_t(x,\ t)\mathrm{d}x = -\int_{\partial\Omega} \rho\boldsymbol{u}\cdot\boldsymbol{n}\mathrm{d}S \tag{9}$$

From Stokes Formula, equation (9) can also be written as

$$\int_\Omega [\rho_t + (\rho u)_x]\,\mathrm{d}x = 0 \tag{10}$$

Due to the arbitrariness of Ω, equation (10) is equivalent to equation (1).

Equation (2) is the momentum-conservation equation, momentum conservation refers to the change in fluid momentum per unit time is always equal to the magnitude of the impact from external force impact on the fluid. By combining the classical fluid dynamics momentum conservation

equation with the actual traffic scenario (where the traffic flow is driven by itself rather than external forces), the following traffic flow conservation equation can be obtained:

$$\int_{\Omega} \frac{\partial}{\partial t}(\rho u)_x \mathrm{d}x = -\int_{\partial\Omega} (\rho u)_x (\boldsymbol{u}\cdot\boldsymbol{n})\mathrm{d}S + \int_{\partial\Omega} \boldsymbol{F}\cdot\boldsymbol{n}\mathrm{d}S \quad (11)$$

where $\boldsymbol{F}$ is the tension on the outer surface of Ω. In non-Newtonian fluid dynamics, $\boldsymbol{F}$ is usually affected by pressure and viscosity, so $\boldsymbol{F}$ is usually expressed as:

$$\boldsymbol{F} = -\boldsymbol{\Gamma}(\rho,\ u_x) + \boldsymbol{P}(\rho) \quad (12)$$

where Γ is the shear force and $\boldsymbol{P}$ is the pressure. Due to the compressibility of the micro clusters, namely the vehicle area in the front and rear of the lane in this scenario, traffic pressure must depend on the density of traffic flow. As the density of traffic increases/decreases, the traffic pressure should also increase/decrease. Based on the above considerations, equation (3) provides a specific expression of traffic pressure. In addition, the characteristics of shear thinning and thickening in non-Newtonian flows have been considered, and a specific expression of shear force has been provided through equation (4). Corresponding to the conventions of classical fluid mechanics equation theory, equations (3) and (4) can be collectively referred to as equations of state. By combining equations (4), (12), (11) with the arbitrariness of Ω, (2) can be obtained from the Stokes Formula.

Equation (5) is the initial condition, it is the initialization of traffic density and traffic speed values at the initial time point. The initial density of traffic flow must be non-negative. Here it is assumed that the initial speed of the traffic flow is 0 without losing generality, but its value can also be adjusted according to the traffic scenario. Equation (6) is the boundary condition, and it is assumed that the speeds at both the initial and final points are zero, which can comprehensively demonstrate both congestion and clear state situations. Of course, the assumptions here are general, and in fact, the boundary values can be adjusted arbitrarily without affecting the selection of subsequent solving methods.

B. MODEL DISCUSSION

There are three important issues that need to be discussed regarding the basic idea of the model proposed in section III-A.

(1) Non-Newtonian flow refers to a shear force that is not proportional to the shear velocity u_x. If it is proportional, it is Newtonian flow, and this stable proportional constant is generally referred to as the viscosity coefficient μ, which is independent of ρ. However, the viscosity coefficient $\mu(\rho)$ of the proposed model depends on density ρ. From equations (2) and (4), it can be seen that the shear force in this article is equal to $\mu(\rho)u_x$. Literature [80] clearly states that if the shear force simultaneously depends on ρ and u_x, the shear force is not proportional to the shear speed u_x, which means that when u_x is increasing/decreasing, the density ρ and the viscosity coefficient μ decreases/increases, so the shear force does not increase/decrease with u_x. As known from literature [80], under the joint action of ρ and u_x, non-Newtonian flow can be generally divided into shear thinning flow or shear thickening flow. Shear thinning flow refers to the phenomenon where the viscosity of non-Newtonian fluids decreases with increasing shear rate; shear thickening flow refers to the phenomenon where the viscosity of non-Newtonian fluids increases with a decrease in shear rate.

(2) When the traffic flow density is constant, it is compatible with the model proposed in this section. From the perspective of fluid mechanics, the movement of traffic flow in the lane can be seen as the movement of liquid in the channel, as the boundaries are fixed. Liquid with constant density is equivalent to ideal liquid, which moves steadily in the channel and has an equal flow speed through each cross-section. From the perspective of this paper, the surface perpendicular to the road width can be considered as a cross-section, and the traffic flow passing through each cross-section is also equal. In fluid mechanics, when the flow rate is fixed, the flow rate is inversely proportional to the cross-sectional area. For the issue in this paper, as the road width is fixed and the vehicle height has an upper limit, the cross-sectional area is a constant. Thus, under the same traffic flow, the traffic flow speed is also a constant. Substitute the two constants of traffic flow density and speed into main equations (1) and (2), since it is needed to take the derivative of density and speed with respect to t and x, both sides of the equation sign collapse to 0, and the equation system remains valid.

(3) From the perspective of non-Newtonian fluid dynamics, there are two extreme situations in the model proposed in this section: one is that the initial density contains a vacuum, which corresponds to a traffic scenario where there are no vehicles on the road at the initial moment; the other assumption is that the length of the road is not finite. In the study of non-Newtonian fluid dynamics, it is often difficult to prove the existence of solutions for the above two types of problems. However, literature [81] has proven the existence of solutions for non-Newtonian models that are more complex in shear force term than the model proposed in this section and consider vacuum and full space difficulties. The expression of the shear force term in the model proposed in this paper is much simpler than that in literature [81], and the existence of the solution in this model can be fully demonstrated using the estimation methods and inverse section techniques involved in literature [81].

IV. SOLVING COMPRESSIBLE NON-NEWTONIAN TRAFFIC FLOW MODEL BASED ON PIRNN

As discussed in Section II-C, most of the existing PDEs for traffic flow are solved by using FEM, however, finite element grids in FEM require higher computational costs and larger storage space, have multiple constraints, lack robustness, and are prone to curse of dimensionality in high-dimensional situations. And as discussed in Section II-D, although using PINN to solve PDEs has become a cutting-edge research direction, there is very little literature on the application of PINN to solving traffic flow PDEs. In order to overcome the

shortcomings of the approximation of the traditional activation function in PINN, rational activation function is used to replace it in this paper and thus PIRNN is formed. And for the first time, PIRNN was used to solve the PDEs of traffic flow, moreover, a concise and efficient NHAGD method is used to improve network training speed for the first time.

A. RATIONAL ACTIVATION FUNCTION

In the framework of the neurons of ANN, the role of activation function is to put the weighted sum into a nonlinear function for nonlinear transformation. Its essence is that the weighted sum can be regarded as a linear hyperplane, which divides spatial data into two categories and can be regarded as a binary linear classifier. But most practical problems are nonlinear, and linear classifier is not of universal significance in application. Therefore, activation function is needed to make linear classifier nonlinear, especially in DL architecture, as the selection of nonlinear activation function is very important and significantly affects the performance of NN. The ideal activation function needs to satisfy many conditions, such as nonlinearity, unsaturation, and almost differentiable everywhere.

The common activation function in the field of DL can be roughly divided into 2 categories: one is smooth activation function, such as Hyperbolic tangent, Sigmoid, Logistic, etc., but both sides of the functions are saturated, that is, the derivatives on both sides tend to zero, so it is easy to produce the problem of gradient vanishing in the training process; the other is polynomial activation function, but they also have the problems of numerical instability and poor approximation to non-smooth function. In recent years, the most popular choice of activation function is rectified linear unit (ReLU). Many literatures have discussed its advantages from the perspective of approximation theory [82], [83], [84]. However, the drawback of ReLU is also very obvious, as it has a dead zone on the left side of its function. In order to overcome its shortcomings, many improved forms of ReLU have emerged in recent years, such as parametric ReLU (PReLU) [85], exponential linear unit (ELU) [86], Leaky ReLU [87], scaled exponential linear unit (SELU) [88], etc. The biggest drawback of these empirical driven improvement strategies is the lack of rigorous statements and proofs of approximation theory.

In the NN used in this paper, rational activation functions will be used to replace the traditional activation function, as the NN based on rational activation function have been proved to have superior approximation ability and lower training cost than the NN based on ReLU and its variants via rigorous approximation theory, a large number of theoretical deduction and practical applications [89], [90], [91].

Rational activation function is composed of rational functions with trainable coefficients a_i and b_j, and its form is as follows:

$$\sigma(x) = \frac{\sum_{i=0}^{\zeta_1} a_i x^i}{\sum_{j=0}^{\zeta_2} b_j x^j} \tag{13}$$

where ζ_1 and ζ_2 are the polynomial degrees of the numerator and denominator respectively. Equation (13) has rigorous theoretical deduction and expression in literatures [89], [90], [91]. Rational activation function is essentially functions obtained by dividing two trainable polynomial coefficients, which is a new type of nonlinear activation function for NN. One of the main purposes of this paper is to use the strong approximation ability of rational NN to improve the training performance of the PINN network framework and simulate physical constraints in a fidelity manner. And the framework of replacing traditional PINN activation function with rational activation functions proposed in this paper is called PIRNN.

B. NHAGD

The loss function of PIRNN used in this paper is a strongly nonlinear non-convex function. It is difficult to obtain the global optimal solution by using the traditional gradient descent (GD) method or stochastic gradient descent (SGD) method, moreover, as the network has many parameters, the above methods will produce intense sawtooth oscillation when approaching the local optimal solution, and the search speed is slow. Thus, accelerated optimization technology is used to accelerate the process of finding global optimal solution. The most classical acceleration gradient method (AGM) is proposed by Nesterov [92], and the very method has been extended later on [93], [94], and [95], however, it only works for strong convex function. In recent years, AGM has been extended to non-convex optimization problems [96], [97], [98], [99], [100], [101], [102], but those methods often introduce a large number of hyperparameter, and the optimal selection of hyperparameter often costs extra time. Essentially, non-convex optimization problems are still open problems at present, and there is no recognized and clear technical roadmap. The proposal of a specific method cannot be applied to all non-convex problems.

Another main purpose of this paper is to provide a concise and efficient non-convex optimization method to assist NN operation. Therefore, inspired by literature [103], in this paper, the global optimization advantages of the noise gradient descent method have been combined with the fast acceleration optimization advantages of the heavy ball method, and a NHAGD method has been proposed for the first time. The iterative format of its network parameters is as follows:

$$\theta_{k+1} = \theta_k - \alpha \nabla f(\theta_k) + \eta(\theta_k - \theta_{k-1}) + \xi \tag{14}$$

where α is the step size of network parameter in PINN, η is the heavy ball acceleration coefficient, and ξ is the standard Gaussian noise.

This method can not only break out of the trap of local optimal solution during the algorithm optimization process, but also accelerate the optimization process. The θ_k–θ_{k-1} term is the acceleration in the current descent direction, and η is used to adjust the acceleration amplitude. NHAGD can solve the disadvantages of NN in solving PDEs mentioned in Section II-D.

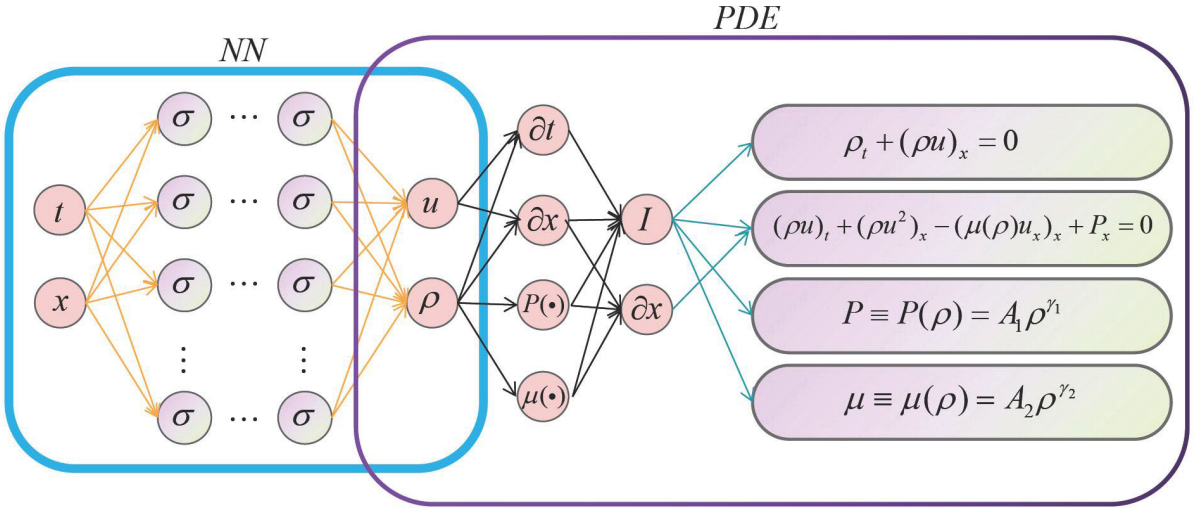

FIGURE 1. The structure diagram of PIRNN for solving compressible non-Newtonian traffic flow PDEs.

C. PIRNN STRUCTURE FOR SOLVING COMPRESSIBLE NON-NEWTONIAN TRAFFIC FLOW PDES

This section gives the PIRNN structure for solving compressible non-Newtonian traffic flow PDEs and the construction of loss function. The structure diagram of PIRNN is shown in Figure 1. Each set of data used for training has an input of time value t and micro cluster coordinate value x, corresponding to its μ, ρ values. The process of numerical experiment training is to learn the μ, ρ values when t, x values are given. The blue part in Figure 1 is PIRNN, which is a 2-input node, 2-output node structure with 6 intermediate layers of 6 nodes.

For the construction of loss function, the following auxiliary definitions should be given first:

$$h_1 = \rho_t + (\rho u)_x \tag{15}$$

$$h_2 = (\rho u)_t + (\rho u^2)_x - (\mu(\rho)u_x)_x + P_x \tag{16}$$

$$h_3 = \rho(x,\ 0) - \rho_0 \tag{17}$$

$$h_4 = u(x,\ 0) \tag{18}$$

$$h_5 = u(\kappa_1,\ t) - u(\kappa_2,\ t) \tag{19}$$

$$h_6 = \frac{\partial[\rho_t + (\rho u)_x]}{\partial t} \tag{20}$$

$$h_7 = \frac{\partial[\rho_t + (\rho u)_x]}{\partial x} \tag{21}$$

$$h_8 = \frac{\partial[(\rho u)_t + (\rho u^2)_x - (\mu(\rho)u_x)_x + P_x]}{\partial t} \tag{22}$$

$$h_9 = \frac{\partial[(\rho u)_t + (\rho u^2)_x - (\mu(\rho)u_x)_x + P_x]}{\partial x} \tag{23}$$

$$\begin{aligned} loss = {} & \frac{1}{2N}\sum_{i=1}^{N}(\rho_i^t - \rho_i^p)^2 + \frac{1}{2N}\sum_{i=1}^{N}(u_i^t - u_i^p)^2 \\ & + \frac{1}{2N}\sum_{i=1}^{N}(P_i^t - A_1(\rho_i^p)^{\gamma_1})^2 \\ & + \frac{1}{2N}\sum_{i=1}^{N}(\mu_i^t - A_2(\rho_i^p)^{\gamma_2})^2 \end{aligned} \tag{24}$$

Furthermore, the form of total loss function can be given as:

$$loss_{total} = \omega_1 loss + \sum_{i=1}^{9}\omega_{i+1} loss_{h_i} + \omega_{11}||\theta||_2^2 \tag{25}$$

where

$$loss_{h_i} = \frac{1}{N}\sum_{i=1}^{N}||h_i||^2 \tag{26}$$

As mentioned before in Section IV-A, The NN model used in the PIRNN framework proposed in this paper is a rational neural network, that is, the traditional network activation function is replaced by rational activation function. The operation of lower order and higher order partial derivative in the loss function can be realized through automatic differentiation. The optimizer of the total loss function is NHAGD proposed in this paper, where *loss* is the sum of the errors between the predicted values and the true values of physical quantities at each data point. $loss_{h1}$ and $loss_{h2}$ are the physical rule constraint losses of the 2 main equations (1) and (2). It is hoped that under the norm metric, the predicted values of the 2 primary equations given by the network are as close to 0 as possible. Similarly, $loss_{h3}$, $loss_{h4}$, and $loss_{h5}$ represent the physical rule constraint losses for initial and boundary conditions. In order to further strengthen the network training effect, even if the rules learned by the network are closer to the physical rules, four sub loss functions $loss_{h6}$, $loss_{h7}$, $loss_{h8}$, and $loss_{h9}$ are set. The idea is that since the 2 primary equation are 0, their partial derivative of each variable are naturally 0. The advantage of doing so is that it cannot only improve the fidelity of the network in learning physical rules, but also eliminate a large number of generalized solutions with low fidelity. ω_i $(i = 1, 2, \ldots, 10)$ is the weight coefficient of each sub loss function. The value of these hyperparameter during network training can be adjusted according to the importance of the sub loss function and the actual effect of network

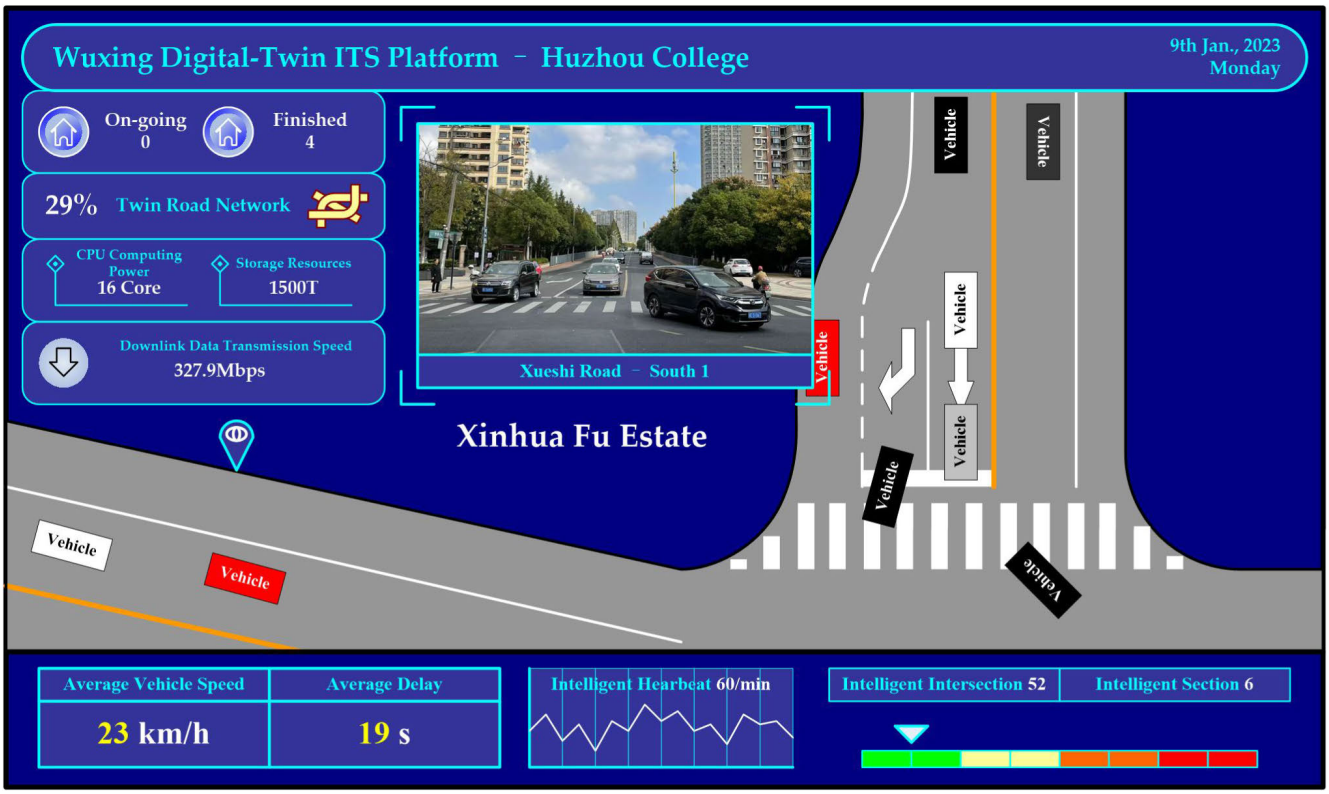

FIGURE 2. Real-time traffic analysis digital twin platform for numerical experiment.

training. To avoid overfitting during network training, the L2 regularization term $||\theta||_2^2$ has been added in equation (25), it is multiplied by the weight hyperparameter ω_{11} so as to adjust its influence, where θ is the network parameter.

Bayesian optimization method is used here to optimize the hyperparameters in network models. From the perspective of hyperparameters, due to the complex stacking of network layers, the specific form of the optimization objective function and its derivatives are unknown, and its essence is a black-box optimization problem. However, this problem is exactly the problem that Bayesian optimization method is good at solving. To solve hyperparameters, the following settings are made to Bayesian optimization method: firstly, the kernel function of the Bayesian linear regression part in the Bayesian optimization method is set to a Gaussian kernel function; secondly, the sampling function in Bayesian optimization methods is set as ''Probability of improvement''.

V. NUMERICAL EXPERIMENT

In order to verify the accuracy of the methodology proposed in this paper in explaining traffic flow, and considering that the non-Newtonian fluid model proposed in this paper is a 1D compressible model, the applicability of the model can only handle the viscoelastic and pressure effects of non-Newtonian fluid along the lateral direction (i.e. the direction of traffic flow). Therefore, in this section, a 530m long two-way single lane road in Wuxing District, Huzhou City, Zhejiang Province, China has been chosen for numerical experiment. The numerical analysis process relies on the research team and the established real-time intelligent transportation analysis digital twin platform, whose interface is shown in Figure 2. This platform can fully utilize the digital camera information of all main roads in Wuxing District, Huzhou, and reproduce its virtual scene based on real-time road traffic scenes. It can also serve as a basic data base for real-time traffic parameter analysis according to user definitions. Due to the fact that parameters such as viscosity and shear force in non-Newtonian fluid cannot be directly determined with the naked eye, calculations need to be made based on experience. Therefore, the advantage of digitizing actual traffic scenes using this platform can provide real-time parameters of observed traffic flows according to compressible non-Newtonian fluid theory.

In actual numerical experiments, 10000 sets of sample data under congestion conditions were intercepted and analyzed, the model was trained by using a 100-round 10-fold cross validation method. Considering the vehicle motion characteristics in the actual road scene of numerical experiments, as well as the micro cluster characteristics in non-Newtonian fluid, a distance of 10 meters is defined as the critical value to determine whether the vehicles belong to the same compressible micro cluster. Each set of data applied to numerical experiments is collected in seconds from the experimental road site. After twinning the scene, the average speed u of

TABLE 2. Error results of the 50th round of 10-fold cross validation of the PIRNN method.

Number of experiments for the 50th 10-fold cross validation	Variable	Training set error			Test set error		
		RMSE (%)	MAE (%)	MAPE (%)	RMSE (%)	MAE (%)	MAPE (%)
1	ρ	4.29	3.37	0.0130	5.81	4.20	0.0228
	u	6.83	4.01	0.0265	2.19	1.43	0.0124
	P	6.79	5.00	0.0301	6.72	4.64	0.0233
	μ	1.53	1.29	0.0096	1.73	1.16	0.0069
2	ρ	6.33	5.61	0.0279	6.95	5.02	0.0229
	u	3.68	3.56	0.0160	2.01	1.07	0.0076
	P	6.81	6.03	0.0281	6.90	6.62	0.0232
	μ	2.26	5.05	0.0111	3.22	2.60	0.0194
3	ρ	5.59	5.34	0.0288	3.61	3.21	0.0202
	u	4.51	4.02	0.0278	1.27	0.89	0.0063
	P	6.48	5.95	0.0183	5.15	3.13	0.0201
	μ	5.54	5.23	0.0170	5.71	4.02	0.0218
4	ρ	7.71	7.41	0.0230	3.97	3.71	0.0184
	u	2.35	2.13	0.0070	1.50	1.29	0.0064
	P	6.24	5.56	0.0280	7.80	6.53	0.0255
	μ	5.68	4.22	0.0179	3.25	0.20	0.0150
5	ρ	1.27	1.07	0.0281	1.88	1.69	0.0111
	u	4.74	0.75	0.0260	1.78	1.61	0.0101
	P	2.29	2.18	0.0269	1.50	1.15	0.0179
	μ	1.92	1.32	0.0164	1.24	0.72	0.0219
6	ρ	4.94	3.11	0.0281	4.32	3.87	0.0200
	u	5.23	5.03	0.0213	7.97	6.69	0.0261
	P	6.36	5.91	0.0157	2.41	2.33	0.0170
	μ	6.85	5.70	0.0292	4.68	3.82	0.0182
7	ρ	6.63	5.35	0.0280	7.26	5.70	0.0241
	u	0.78	0.71	0.0036	0.96	0.21	0.0032
	P	2.55	1.72	0.0267	4.71	4.31	0.0208
	μ	7.77	5.42	0.0324	5.26	3.70	0.0168
8	ρ	2.63	2.23	0.0096	2.41	0.73	0.0121
	u	1.50	1.04	0.0092	2.11	3.41	0.0115
	P	5.53	4.53	0.0261	1.02	4.44	0.0120
	μ	4.37	3.12	0.0172	4.60	2.00	0.0188
9	ρ	7.75	6.73	0.0282	7.02	6.77	0.0252
	u	6.11	6.91	0.0254	7.16	6.56	0.0240
	P	6.23	5.53	0.0222	7.01	5.03	0.0232
	μ	7.44	5.96	0.0283	6.95	4.45	0.0212
10	ρ	2.33	2.31	0.0081	2.41	1.00	0.0129
	u	3.20	3.00	0.0256	3.12	1.44	0.0166
	P	1.32	0.62	0.0065	5.72	2.61	0.0211
	μ	4.87	3.09	0.0171	3.33	3.31	0.0196

sample data as non-Newtonian fluid micro clusters can be automatically perceived, and the vehicle density ρ, pressure P and viscosity coefficient μ of micro clusters can also be analyzed out by the system based on the definition of non-Newtonian fluid, which strictly correspond to the parameters learned by the PIRNN network shown in Figure 1.

As the 10-fold cross validation method mentioned above has been used in the training phase of the entire PIRNN network to train and test the performance, it can also solve the problem of overfitting. The dataset consisting 10000 sets of data is divided into 10 parts, 9 of them is used by taking turns as training data, and 1 of them is used as test data for the experiment. Each experiment will result in corresponding errors. In order to fully verify the effectiveness of the algorithm proposed in this paper, root mean square error (RMSE), mean absolute error (MAE), and mean absolute percentage error (MAPE) have been used as measurement indicators. The average values of the 3 measurement indicators for the results of the 10th round are used as estimates of algorithm accuracy, and 100 rounds of 10-fold cross validation are conducted. Here, the results of the 50th round of 10-fold cross validation are taken as an example, which is shown in Table 2.

By taking the mean of the 3 measurement indicators of these 10 results, the average error of the 50th round 10-fold cross validation can be obtained, as shown in Table 3.

TABLE 3. Average error of the 50th round of 10-fold cross validation of the PIRNN method.

Variable	Training set error			Test set error		
	RMSE (%)	MAE (%)	MAPE (%)	RMSE (%)	MAE (%)	MAPE (%)
ρ	4.95	4.25	0.0223	4.56	3.59	0.0190
u	3.89	3.12	0.0188	3.01	2.46	0.0124
P	5.06	4.30	0.0229	4.89	4.08	0.0204
μ	4.82	4.04	0.0196	4.00	2.60	0.0180

The average error can also be obtained by using the same method for the other 99 rounds 10-fold cross validation tests. By taking the average error of the 100-round 10-fold cross validation tests, the results in Table 4 can be obtained.

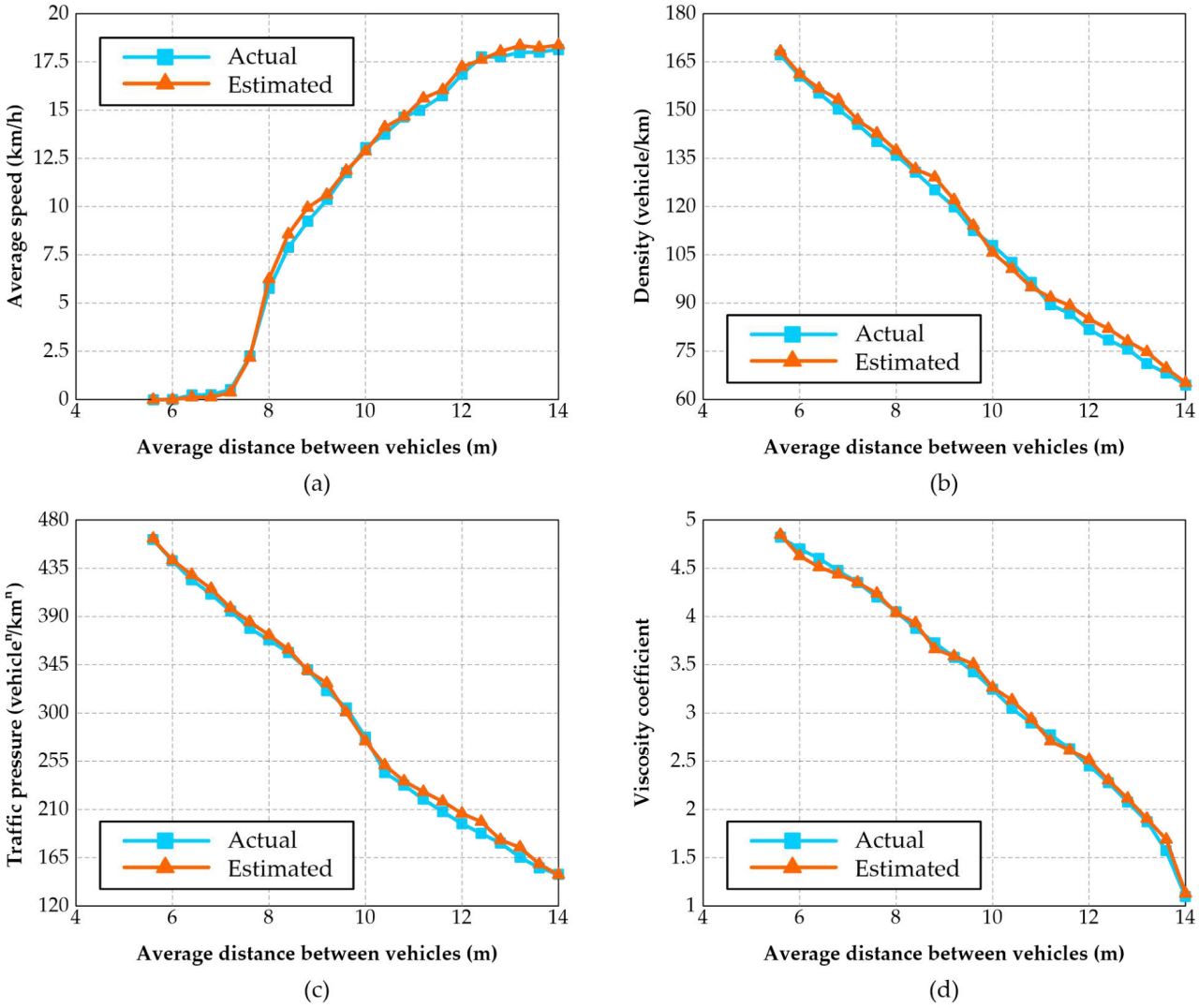

FIGURE 3. The relationship between the average distance of vehicles in micro cluster and non-Newtonian traffic flow characteristic parameters.

TABLE 4. Average error of 100-round 10-fold cross validation of the PIRNN method.

Variable	Training set error			Test set error		
	RMSE (%)	MAE (%)	MAPE (%)	RMSE (%)	MAE (%)	MAPE (%)
ρ	4.78	4.21	0.0211	4.45	3.52	0.0182
u	3.81	3.14	0.0182	3.02	2.40	0.0117
P	4.96	4.22	0.0222	4.83	4.10	0.0200
μ	4.73	4.09	0.0193	4.03	2.61	0.0184

Then, by taking the mean of Table 4 by the number of variables, an intuitive overall error can be obtained, as shown in Table 5.

In order to facilitate the comparison of various methods, L2 regularization term has been added to the loss function of PINN with ReLU activation function, and 100-round 10-fold cross validation method has also been used for training. By using the same method above, the overall error of RMSE, MAE and MAPE can also be acquired. Furthermore, RMSE, MAE, and MAPE have also been used as measurement indicators for error estimation of the traditional FEM method. In this way, a comparison of the overall error of each method can be obtained, as shown in Table 6.

TABLE 5. Overall error of the PIRNN method.

Training set error			Test set error		
RMSE (%)	MAE (%)	MAPE (%)	RMSE (%)	MAE (%)	MAPE (%)
4.57	3.92	0.0202	4.08	3.16	0.0171

It can be observed that the overall error of the PIRNN method, including RMSE, MAE, and MAPE, is significantly smaller than the values of PINN (ReLU) and FEM. And it can be seen that the rational activation functions in PIRNN have stronger fitting ability than the traditional activation function, and the NHAGD method in PIRNN has stronger

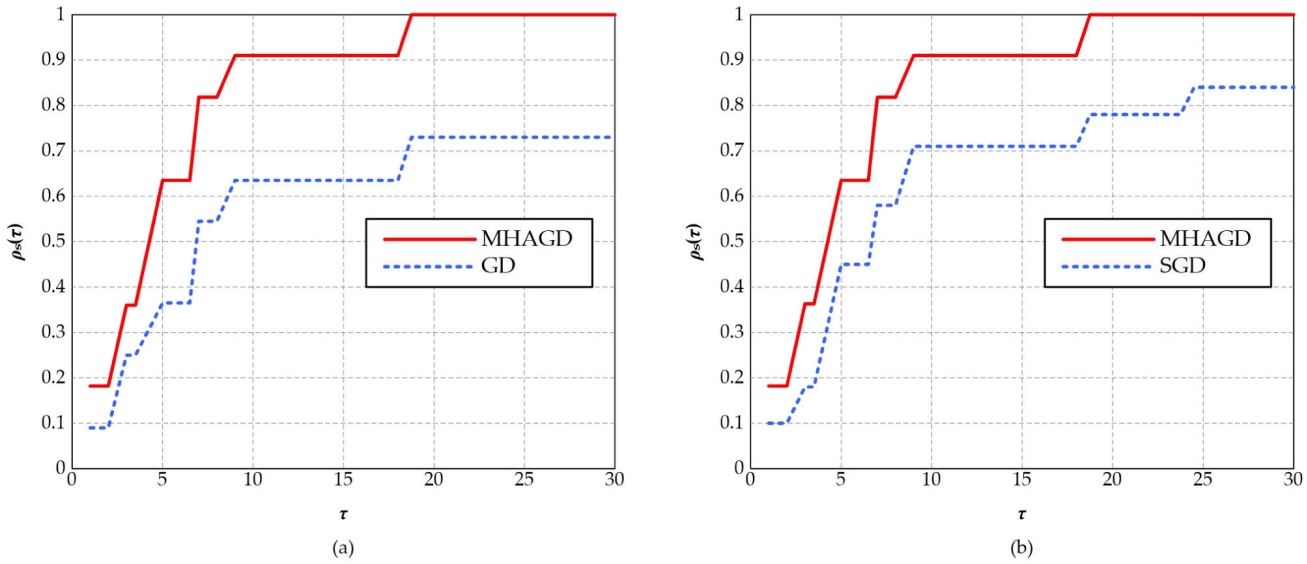

FIGURE 4. Performance of CPU time for MHAGD, GD and SGD based non-Newtonian fluid model solution.

TABLE 6. Comparison of overall errors between PIRNN, PINN(ReLU) and FEM.

Method	Training set error			Test set error		
	RMSE (%)	MAE (%)	MAPE (%)	RMSE (%)	MAE (%)	MAPE (%)
PIRNN	4.57	3.92	0.0202	4.08	3.16	0.0171
PINN (ReLU)	7.48	7.16	0.0829	7.31	6.50	0.0781
FEM	8.38	7.88	0.1552	8.18	7.58	0.1388

optimization accuracy than the traditional optimizer for the parameter optimization of non convex loss function. It can also be observed that the RMSE, MAE, and MAPE indicators of each variable in the PIRNN method were relatively stable in terms of both training and testing set errors. This further indicates that the PIRNN using rational activation functions exhibits extremely robust network fitting ability, which is consistent with the theoretical derivation of rational activation functions discussed in literatures [89], [90], [91].

Figure 3 shows the true and predicted relationships between the values of vehicle average speed, density, traffic pressure, viscosity coefficient, and the value of average distance Δx between vehicles in the micro cluster under the condition of congestion when the average distance between vehicles is close to 4 meters, namely the condition of non-Newtonian shear thickening fluid. It can be seen that with the average distance Δx of vehicles in the micro cluster decreases, the traffic flow speed u decreases, but the density ρ, pressure P and viscosity coefficient μ are getting bigger and bigger. Moreover, Figure 3 also shows the condition of clear state when the average distance between vehicle is close to 14 meters, namely the condition of non-Newtonian shear thinning fluid. Contrary to the previous status, with the average distance Δx of vehicles in the micro cluster increases, the traffic flow speed u increases, but the density ρ, pressure P and viscosity coefficient μ are getting smaller and smaller. Due to the power law relationship between pressure P, viscosity coefficient μ and density ρ in non-Newtonian fluid, the changes of P and μ are slightly more obvious compared to ρ. It can be seen that the compressible non-Newtonian fluid model proposed in this paper can accurately estimate parameters such as speed and density of real traffic flow.

In order to verify the efficiency of the proposed compressible non-Newtonian fluid model solved by PIRNN with NHAGD fused in its optimization process, the CPU time efficiency and iteration efficiency of PIRNN using NHAGD as parameter optimization method were compared with GD method SGD method under the same computational conditions. In the comparison, the classical performance evaluation index $\rho_s(\tau)$ in the field of optimization proposed by Dolan et al. and further applied by Li et al. has been introduced [104], [105]. In essence, $\rho_s(\tau)$ is generated by running a solver on a set of problems and recording the information of interest, and it is just a probability that the solver can defeat other solvers. The results are based on the number of iterations and CPU time respectively. For the convenience of expression, the number of iterations is recorded as NIT. As shown in Figure 4 and Figure 5, the higher the algorithm performance curve in those figures, the better performance of the corresponding model is, and it can be clearly seen that, the performance of NHAGD based PIRNN out performs traditional GD or SGD based PIRNN in solving compressible non-Newtonian fluid road traffic flow PDEs.

Moreover, in order to verify the effectiveness of the proposed traffic flow model in this paper, it has been compared with classic models proposed by Lighthill et al. [70], Pipes [71], Payne [72], Whitham [73], Phillips [74], Wu [75], Hoogendoorn et al. [76], and Helbing et al. [77], as well as the

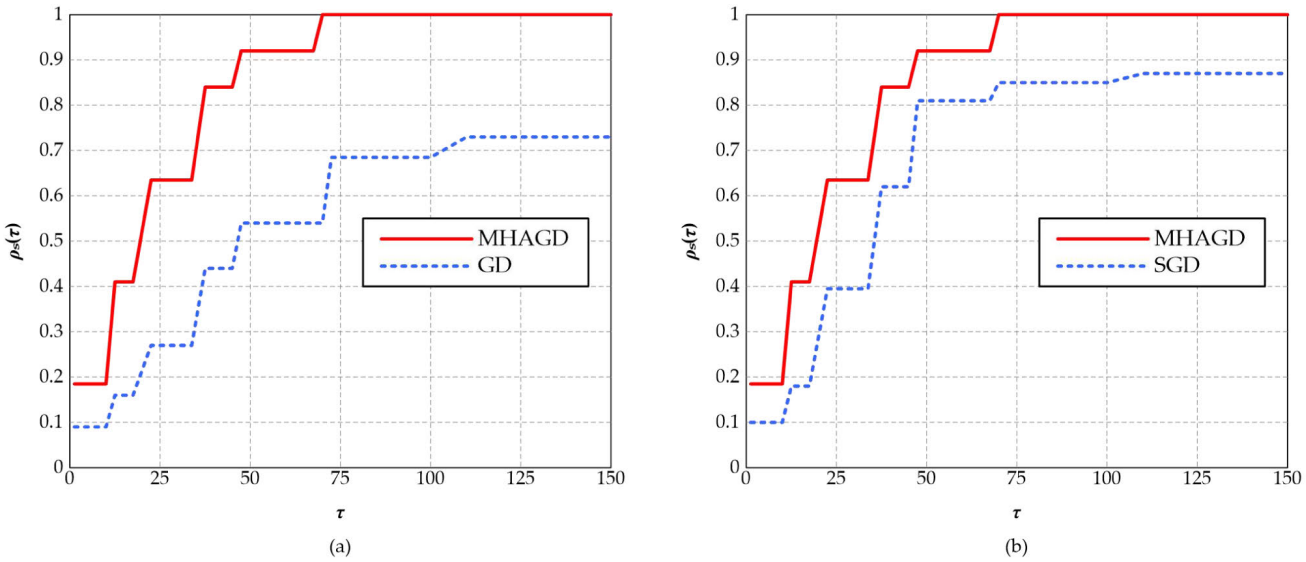

FIGURE 5. Performance of NIT time for MHAGD, GD and SGD based non-Newtonian fluid model solution.

TABLE 7. Comparison of RMSE, MAE, and MAPE between various models.

Model	Variable	Training set error			Test set error		
		RMSE (%)	MAE (%)	MAPE (%)	RMSE (%)	MAE (%)	MAPE (%)
Model proposed in this paper	ρ	4.78	4.21	0.0211	4.45	3.52	0.0182
	u	3.81	3.14	0.0182	3.02	2.40	0.0117
Model in [70]	ρ	13.23	13.16	0.2361	12.98	12.82	0.2269
	u	12.86	13.14	0.2352	12.36	12.27	0.2258
Model in [71]	ρ	13.21	13.16	0.2351	13.02	12.94	0.2263
	u	12.37	12.28	0.2298	12.22	12.13	0.2279
Model in [72]	ρ	11.96	11.87	0.2097	11.86	11.76	0.2088
	u	11.12	11.03	0.2089	10.98	10.77	0.2071
Model in [73]	ρ	10.73	10.69	0.1976	10.63	10.59	0.1958
	u	10.45	10.32	0.1955	10.15	10.09	0.1941
Model in [74]	ρ	7.65	7.55	0.0935	7.45	7.36	0.0888
	u	6.89	6.56	0.0827	6.77	6.43	0.0816
Model in [75]	ρ	9.36	9.23	0.1423	9.18	9.04	0.1421
	u	9.12	9.08	0.1389	8.99	8.83	0.1375
Model in [76]	ρ	9.21	9.13	0.1412	9.17	9.02	0.1400
	u	8.54	8.41	0.1267	8.44	8.31	0.1253
Model in [77]	ρ	8.88	8.75	0.1288	8.72	8.63	0.1278
	u	8.31	8.22	0.1231	8.03	7.98	0.1036
Hyperbolic traffic flow model in [69]	ρ	5.36	5.29	0.0352	5.35	5.31	0.0345
	u	5.21	5.17	0.0314	5.14	5.11	0.0312
VFFM in [78]	ρ	5.18	5.12	0.0301	5.09	5.06	0.0296
	u	5.02	5.00	0.0287	5.00	4.97	0.0273

hyperbolic traffic flow model [69] and the VFFM [78] proposed during recent years, so as to measure the approximation between the predicted values of each model and the true values. For the sake of fairness, PRINN has been uniformly used as the solver for the differential equation system of the above models, and the same data collected has been used to train the network by employing 100 rounds of 10-fold cross validation method. Standardized indicators RMSE, MAE and MAPE have still been used to evaluate the predictive ability of the model. Due to the fact that most of the above models only use traffic flow density and speed to depict traffic flow phenomena, they are not as precise as the model proposed in this paper in depicting traffic flow, as the model proposed in this paper introduces compressible traffic pressure terms and viscosity coefficient terms. And by considering the matter of fact mentioned above, traffic flow density has only been compared with traffic flow speed. As shown in Table 7, the model proposed in this paper, hyperbolic traffic flow model, and VFFM have smaller errors due to their more refined traffic flow characterization compared to other models. And to be specific, the compressible non-Newtonian traffic flow model proposed in this paper is closer to the viscosity characteristics of traffic flow and better reflects the compression characteristics of the vehicle domain than the hyperbolic traffic flow

model and VFFM under the incompressible Newtonian flow framework, so the error performance is better.

VI. CONCLUSION

This paper proposes an urban road traffic flow analysis model based on compressible non-Newtonian fluid and solvable by PIRNN. Firstly, this is the first time that compressible non-Newtonian fluid has been applied to traffic flow analysis within the author's cognitive scope, compared to non-compressible non-Newtonian fluid, the particle clusters formed between vehicles described by it are closer to the actual characteristics of traffic flow; secondly, different from FEM method, this paper uses PIRNN to solve the PDEs of the proposed non-Newtonian fluid model, the solution process fully considers the shortcomings of NN-based algorithms that have been pointed out by previous scholars in solving PDEs with low efficiency. By introducing rational activation function and NHAGD to NN, the learning and training speed of PIRNN is guaranteed.

From the coordinate dimension of traffic flow, the compressible non-Newtonian fluid based model proposed in this paper can only explain 1D scenarios, which has limitations for analyzing the phenomena generated in actual urban road traffic. In subsequent research, it is hoped to study different traffic scenarios, such as introducing non-Newtonian fluid PDEs such as pipeline fluid equations, electromagnetic fluid equations, quantum fluid equations, etc. into the field of traffic fluid PDEs. In this way, the research scenarios can be expanded to multi-dimensional spatial situations, multi lane situations, multi-dimensional random traffic scenarios, and different intersection situations.

Moreover, from the perspective of the application of artificial intelligence in the field of traffic flow analysis, reinforcement learning (RL), or even imitation learning (IL) algorithms can be introduced into this research field in the future, which can be used to solve the intelligent guidance and control of traffic flow in special emergency situations. Such idea just comes from the field of intelligent fluids related to this paper, and its purpose is to arbitrarily control the shape of fluid through electrical or magnetic signals. Of course, knowledge distillation can also be introduced into this field, with the main purpose of efficiently fusing and compressing multi task traffic flow description and control models, and obtaining a compressed versatile traffic flow model that can handle different traffic scenes.

APPENDIX A
ABBREVIATIONS

1D	One dimensional
AGM	Acceleration gradient method
AI	Artificial intelligence
ANN	Artificial neural network
AV	Automated vehicle
CA	Cellular automata
CAV	Connected automated vehicle
DL	Deep learning
ELU	Exponential linear unit
FEM	Finite element method
fPINN	fractional physical-informed neural network
GD	Gradient descent
IL	Imitation learning
MAE	Mean square error
MAPE	Mean absolute percentage error
ML	Machine learning
NHAGD	Noise heavy-ball acceleration gradient descent
NN	Neural network
PDE	Partial differential equation
PINN	Physical-informed neural network
PIRNN	Physical-informed rational neural network
PReLU	Parametric rectified linear unit
PSO	Particle swarm intelligence
ReLU	Rectified linear unit
RL	Reinforcement learning
RMSE	Root mean square error
SELU	Scaled exponential linear unit
SFEM	Smooth finite element method
SGD	Stochastic gradient descent
TTI	Travel time index
VFFM	Virtual fluid-flow-model
VPINN	Variational physical-informed neural network

APPENDIX B
NOMENCLATURE

t	Time
x	Lateral coordinate of traffic flow (coordinate in the flow direction)
ρ	Traffic flow density
$\boldsymbol{u}$	Traffic flow speed
$\boldsymbol{P}$	Traffic pressure
μ	Viscosity coefficient, which is assumed to depend on traffic flow density ρ
A_1	Constant coefficient of traffic pressure
γ_1	Power coefficient of traffic pressure
A_2	Constant coefficient of viscosity function
γ_2	Power coefficient of viscosity function
ρ_0	Initial density
κ_0	Starting point coordinates in boundary conditions
κ_1	Ending point coordinates in boundary conditions
T	Total time length
$\sigma(x)$	Rational activation function
a_i	Trainable coefficients in the numerator of rational activation function
b_j	Trainable coefficients in the denominator of rational activation function
ζ_1	Polynomial degree in the numerator of rational activation function
ζ_2	Polynomial degree in the denominator of rational activation function
ω_i	Weight coefficient of each sub loss function
ρ_i^t	The actual value of traffic flow density of the i-th data

$\boldsymbol{u_i^t}$	The actual value of traffic flow speed of the i-th data
$\boldsymbol{P_i^t}$	The actual value of traffic pressure of the i-th data
μ_i^t	The actual value of viscosity coefficient of the i-th data
ρ_i^p	The predictive value of traffic flow density of the i-th data
$\boldsymbol{u_i^p}$	The predictive value of traffic flow speed of the i-th data
β	Super parameter of Xwish activation function
θ	Network parameter in physical-informed neural network (PINN)
α	Step size of network parameter in PINN
ξ	Standard Gaussian noise
η	Heavy ball acceleration coefficient
f	Objective function
N	Number of data samples
Ω	A segment in traffic flow
$\boldsymbol{n}$	Unit outer normal vector
$\boldsymbol{F}(x,t)$	Tension on Ω outer surface
$\Gamma(\rho, u_x)$	Shear force

REFERENCES

[1] *People's Daily Overseas Edition*. Accessed: May 10, 2023. [Online]. Available: http://paper.people.com.cn/rmrbhwb/html/2022-03/22/node_867.htm
[2] W. Nai, Z. Yang, D. Lin, D. Li, and Y. Xing, "A vehicle path planning algorithm based on mixed policy gradient actor-critic model with random escape term and filter optimization," *J. Math.*, vol. 2022, pp. 1–17, Aug. 2022, doi: 10.1155/2022/3679145.
[3] J. Tian, "The physics and simulation of occupant traffic flow in the case of evacuating public building area," *Transp. Res. D, Transp. Environ.*, vol. 30, pp. 76–85, Jul. 2014, doi: 10.1016/j.trd.2014.05.009.
[4] D. Chen, M. Hu, Y. Ma, and J. Yin, "A network-based dynamic air traffic flow model for short-term en route traffic prediction," *J. Adv. Transp.*, vol. 50, no. 8, pp. 2174–2192, Dec. 2016, doi: 10.1002/atr.1453.
[5] S. Moukir, N. Emad, and S. Baudelocq, "A high performance approach with MATSim for traffic road simulation," in *Proc. 12th Int. Congr. Adv. Appl. Informat. (IIAI-AAI)*, Kanazawa, Japan, Jul. 2022, pp. 679–681, doi: 10.1109/IIAIAAI55812.2022.00140.
[6] P. Zhang, Y. Y. Zhang, F. Lei, G. Zhu, J. Guo, and Y. Quan, "Dynamic traffic flow–dispersion model based on TTI of floating cars," *J. Transp. Eng., A, Syst.*, vol. 143, no. 1, Jan. 2017, Art. no. 04016001, doi: 10.1061/jtepbs.0000001.
[7] S. Wang, N. U. Ahmed, and T. H. Yeap, "Optimum management of urban traffic flow based on a stochastic dynamic model," *IEEE Trans. Intell. Transp. Syst.*, vol. 20, no. 12, pp. 4377–4389, Dec. 2019, doi: 10.1109/TITS.2018.2884463.
[8] F. Yan, J. Qiu, and J. Tian, "An iterative learning identification strategy for nonlinear macroscopic traffic flow model," *Phys. A, Stat. Mech. Appl.*, vol. 604, Oct. 2022, Art. no. 127901, doi: 10.1016/j.physa.2022.127901.
[9] A. Dabiri and B. Kulcsar, "Incident indicators for freeway traffic flow models," *Commun. Transp. Res.*, vol. 2, Apr. 2022, Art. no. 100060.
[10] X. Ni, H. Huang, Y. Liu, K. Liu, M. Wang, and J. Hu, "Study of local traffic flow fluctuation under rainfall and waterlogging with characteristics of dynamic spatiotemporal changes," *J. Transp. Eng., A, Syst.*, vol. 148, no. 7, Jul. 2022, Art. no. 04022039, doi: 10.1061/jtepbs.0000670.
[11] Q. Zhang and S. Liu, "The Riemann problem and a Godunov-type scheme for a traffic flow model on two lanes with two velocities," *Appl. Math. Comput.*, vol. 436, Jan. 2023, Art. no. 127502, doi: 10.1016/j.amc.2022.127502.
[12] C. Jin, V. L. Knoop, R. Jiang, W. Wang, and H. Wang, "Calibration and validation of cellular automaton traffic flow model with empirical and experimental data," *IET Intell. Transp. Syst.*, vol. 12, no. 5, pp. 359–365, Jun. 2018, doi: 10.1049/iet-its.2016.0275.
[13] A. Poole and A. Kotsialos, "METANET validation of the large-scale Manchester ring-road network using gradient-based and particle swarm optimization," *IEEE Trans. Intell. Transp. Syst.*, vol. 19, no. 7, pp. 2055–2065, Jul. 2018, doi: 10.1109/TITS.2017.2724941.
[14] Y. Wang, X. Yu, J. Guo, I. Papamichail, M. Papageorgiou, L. Zhang, S. Hu, Y. Li, and J. Sun, "Macroscopic traffic flow modelling of large-scale freeway networks with field data verification: State-of-the-art review, benchmarking framework, and case studies using METANET," *Transp. Res. C, Emerg. Technol.*, vol. 145, Dec. 2022, Art. no. 103904, doi: 10.1016/j.trc.2022.103904.
[15] Y. Li, S. Zhang, Y. Pan, B. Zhou, and Y. Peng, "Exploring the stability and capacity characteristics of mixed traffic flow with autonomous and human-driven vehicles considering aggressive driving," *J. Adv. Transp.*, vol. 2023, pp. 1–21, Feb. 2023, doi: 10.1155/2023/2578690.
[16] W. Tian, J. Ma, L. Qiu, X. Wang, Z. Lin, C. Luo, Y. Li, and Y. Fang, "The double lanes cell transmission model of mixed traffic flow in urban intelligent network," *Energies*, vol. 16, no. 7, p. 3108, Mar. 2023, doi: 10.3390/en16073108.
[17] H. Mo, X. Hao, H. Zheng, Z. Liu, and D. Wen, "Linguistic dynamic analysis of traffic flow based on social media—A case study," *IEEE Trans. Intell. Transp. Syst.*, vol. 17, no. 9, pp. 2668–2676, Sep. 2016, doi: 10.1109/TITS.2016.2530698.
[18] X. Wang, R. Zeng, F. Zou, F. Huang, and B. Jin, "A highly efficient framework for outlier detection in urban traffic flow," *IET Intell. Transp. Syst.*, vol. 15, no. 12, pp. 1494–1507, Dec. 2021, doi: 10.1049/itr2.12109.
[19] W. Ai, T. Xing, Y. Su, and D. Liu, "Branch analysis of macro-traffic flow model with different driving characteristics in its environment," *IEEE Access*, vol. 9, pp. 164752–164768, 2021, doi: 10.1109/ACCESS.2021.3121139.
[20] P. J. Storm, M. Mandjes, and B. van Arem, "Efficient evaluation of stochastic traffic flow models using Gaussian process approximation," *Transp. Res. B, Methodol.*, vol. 164, pp. 126–144, Oct. 2022, doi: 10.1016/j.trb.2022.08.003.
[21] Y. Yuan, Q. Wang, and X. T. Yang, "Traffic flow modeling with gradual physics regularized learning," *IEEE Trans. Intell. Transp. Syst.*, vol. 23, no. 9, pp. 14649–14660, Sep. 2022, doi: 10.1109/TITS.2021.3131333.
[22] J. Zeng and J. Tang, "Modeling dynamic traffic flow as visibility graphs: A network-scale prediction framework for lane-level traffic flow based on LPR data," *IEEE Trans. Intell. Transp. Syst.*, vol. 24, no. 4, pp. 4173–4188, Apr. 2023, doi: 10.1109/TITS.2022.3231959.
[23] P. T. Griffiths, "Non-newtonian channel flow—Exact solutions," *IMA J. Appl. Math.*, vol. 85, no. 1, pp. 263–279, Feb. 2020, doi: 10.1093/imamat/hxaa005.
[24] P. Gao, "The finite element numerical investigation of free surface Newtonian and non-newtonian fluid flows in the rectangular tanks," *Math. Problems Eng.*, vol. 2020, pp. 1–18, Nov. 2020, doi: 10.1155/2020/7548192.
[25] A. Redfearn and B. Hanson, "A mechanical simulator of Tongue–Palate compression to investigate the oral flow of non-Newtonian fluids," *IEEE/ASME Trans. Mechatronics*, vol. 23, no. 2, pp. 958–965, Apr. 2018, doi: 10.1109/TMECH.2018.2808704.
[26] W. Shi, P. X. Liu, and M. Zheng, "Bleeding simulation with improved visual effects for surgical simulation systems," *IEEE Trans. Syst., Man, Cybern., Syst.*, vol. 51, no. 2, pp. 686–695, Feb. 2021, doi: 10.1109/TSMC.2018.2883406.
[27] M. M. Bhatti, S. M. Sait, and R. Ellahi, "Magnetic nanoparticles for drug delivery through tapered stenosed artery with blood based non-newtonian fluid," *Pharmaceuticals*, vol. 15, no. 11, p. 1352, Nov. 2022, doi: 10.3390/ph15111352.
[28] Y. Zhang, M. N. Smirnova, A. I. Bogdanova, Z. Zhu, and N. N. Smirnov, "Travel time prediction with viscoelastic traffic model," *Appl. Math. Mech.*, vol. 39, no. 12, pp. 1769–1788, Dec. 2018, doi: 10.1007/s10483-018-2400-9.
[29] J. Ma, C. K. Chan, Z. Ye, and Z. Zhu, "Effects of maximum relaxation in viscoelastic traffic flow modeling," *Transp. Res. B, Methodol.*, vol. 113, pp. 143–163, Jul. 2018, doi: 10.1016/j.trb.2018.05.013.
[30] L. Sun, A. Jafaripournimchahi, A. Kornhauser, and W. Hu, "A new higher-order viscous continuum traffic flow model considering driver memory in the era of autonomous and connected vehicles," *Phys. A, Stat. Mech. Appl.*, vol. 547, Jun. 2020, Art. no. 123829, doi: 10.1016/j.physa.2019.123829.

[31] Y. Kang, S. Mao, and Y. Zhang, "Fractional time-varying grey traffic flow model based on viscoelastic fluid and its application," *Transp. Res. B, Methodol.*, vol. 157, pp. 149–174, Mar. 2022, doi: 10.1016/j.trb.2022.01.007.

[32] I. Karafyllis, D. Theodosis, and M. Papageorgiou, "Constructing artificial traffic fluids by designing cruise controllers," *Syst. Control Lett.*, vol. 167, Sep. 2022, Art. no. 105317, doi: 10.1016/j.sysconle.2022.105317.

[33] L. Benninger and O. Sawodny, "Position-dependent fundamental diagram parameterizations in traffic flow modeling on highways," *IFAC-PapersOnLine*, vol. 55, no. 27, pp. 503–508, 2022, doi: 10.1016/j.ifacol.2022.10.562.

[34] S. Shagolshem, B. Bira, and S. Sil, "Conservation laws and some new exact solutions for traffic flow model via symmetry analysis," *Chaos, Solitons Fractals*, vol. 165, Dec. 2022, Art. no. 112779, doi: 10.1016/j.chaos.2022.112779.

[35] R. Stevenson and J. Westerdiep, "Stability of Galerkin discretizations of a mixed space–time variational formulation of parabolic evolution equations," *IMA J. Numer. Anal.*, vol. 41, no. 1, pp. 28–47, Jan. 2020, doi: 10.1093/imanum/drz069.

[36] S. Metzger, "A convergent finite element scheme for a fourth-order liquid crystal model," *IMA J. Numer. Anal.*, vol. 42, no. 1, pp. 440–486, Jan. 2021, doi: 10.1093/imanum/draa069.

[37] A. A. Memon, M. A. Memon, K. Bhatti, T. A. Alkanhal, I. Khan, and A. Khan, "Analysis of power law fluids and the heat distribution on a facing surface of a circular cylinder embedded in rectangular channel fixed with screen: A finite element's analysis," *IEEE Access*, vol. 9, pp. 74719–74728, 2021, doi: 10.1109/ACCESS.2021.3076042.

[38] S. Bilal, N. Z. Khan, I. A. Shah, J. Awrejcewicz, A. Akgül, and M. B. Riaz, "Heat and flow control in cavity with cold circular cylinder placed in non-newtonian fluid by performing finite element simulations," *Coatings*, vol. 12, no. 1, p. 16, Dec. 2021, doi: 10.3390/coatings12010016.

[39] Y. Nawaz, M. S. Arif, K. Abodayeh, and M. Bibi, "Finite element method for non-newtonian radiative Maxwell nanofluid flow under the influence of heat and mass transfer," *Energies*, vol. 15, no. 13, p. 4713, Jun. 2022, doi: 10.3390/en15134713.

[40] E. Hou, F. Wang, U. Nazir, M. Sohail, N. Jabbar, and P. Thounthong, "Dynamics of tri-hybrid nanoparticles in the rheology of pseudo-plastic liquid with Dufour and soret effects," *Micromachines*, vol. 13, no. 2, p. 201, Jan. 2022, doi: 10.3390/mi13020201.

[41] R. Kune, H. S. Naik, B. S. Reddy, and C. Chesneau, "Role of nanoparticles and heat source/sink on MHD flow of cu-H2O nanofluid flow past a vertical plate with soret and Dufour effects," *Math. Comput. Appl.*, vol. 27, no. 6, p. 102, Nov. 2022, doi: 10.3390/mca27060102.

[42] M. Omri, M. Jamal, S. Hussain, L. Kolsi, and C. Maatki, "Conjugate natural convection of a hybrid nanofluid in a cavity filled with porous and non-newtonian layers: The impact of the power law index," *Mathematics*, vol. 10, no. 12, p. 2044, Jun. 2022, doi: 10.3390/math10122044.

[43] R. Frey and V. Köck, "Deep neural network algorithms for parabolic PIDEs and applications in insurance and finance," *Computation*, vol. 10, no. 11, p. 201, Nov. 2022, doi: 10.3390/computation10110201.

[44] A. Sacchetti, B. Bachmann, K. Löffel, U.-M. Künzi, and B. Paoli, "Neural networks to solve partial differential equations: A comparison with finite elements," *IEEE Access*, vol. 10, pp. 32271–32279, 2022, doi: 10.1109/ACCESS.2022.3160186.

[45] N. Wang, H. Chang, and D. Zhang, "Deep-learning-based inverse modeling approaches: A subsurface flow example," *J. Geophys. Res., Solid Earth*, vol. 126, no. 2, Feb. 2021, Art. no. e2020JB020549, doi: 10.1029/2020jb020549.

[46] H. Xu, "DL-PDE: Deep-learning based data-driven discovery of partial differential equations from discrete and noisy data," *Commun. Comput. Phys.*, vol. 29, no. 3, pp. 698–728, Jun. 2021, doi: 10.4208/cicp.oa-2020-0142.

[47] M. Raissi, P. Perdikaris, and G. Em Karniadakis, "Physics informed deep learning (Part I): Data-driven solutions of nonlinear partial differential equations," 2017, *arXiv:1711.10561*.

[48] M. Raissi, P. Perdikaris, and G. E. Karniadakis, "Physics informed deep learning (Part II): Data-driven discovery of nonlinear partial differential equations," 2017, *arXiv:1711.10566*.

[49] S. Moradi, B. Duran, S. E. Azam, and M. Mofid, "Novel physics-informed artificial neural network architectures for system and input identification of structural dynamics PDEs," *Buildings*, vol. 13, no. 3, 2023, Art. no. 650, doi: 10.3390/buildings13030650.

[50] J. Han and A. Jentzen, "Deep learning-based numerical methods for high-dimensional parabolic partial differential equations and backward stochastic differential equations," *Commun. Math. Statist.*, vol. 5, no. 4, pp. 349–380, Dec. 2017, doi: 10.1007/s40304-017-0117-6.

[51] M. A. Nabian and H. Meidani, "A deep learning solution approach for high-dimensional random differential equations," *Probabilistic Eng. Mech.*, vol. 57, pp. 14–25, Jul. 2019, doi: 10.1016/j.probengmech.2019.05.001.

[52] Y. Gao, L. Qian, T. Yao, Z. Mo, J. Zhang, R. Zhang, E. Liu, and Y. Li, "An improved physics-informed neural network algorithm for predicting the phreatic line of seepage," *Adv. Civil Eng.*, vol. 2023, pp. 1–11, Apr. 2023, doi: 10.1155/2023/5499645.

[53] A. Falini, G. A. D'Inverno, M. L. Sampoli, and F. Mazzia, "Splines parameterization of planar domains by physics-informed neural networks," *Mathematics*, vol. 11, no. 10, p. 2406, May 2023, doi: 10.3390/math11102406.

[54] P. Zhi, Y. Wu, C. Qi, T. Zhu, X. Wu, and H. Wu, "Surrogate-based physics-informed neural networks for elliptic partial differential equations," *Mathematics*, vol. 11, no. 12, p. 2723, Jun. 2023, doi: 10.3390/math11122723.

[55] G. Pang, L. Lu, and G. E. Karniadakis, "FPINNs: Fractional physics-informed neural networks," *SIAM J. Sci. Comput.*, vol. 41, no. 4, pp. A2603–A2626, Jan. 2019, doi: 10.1137/18m1229845.

[56] L. Lu, X. Meng, Z. Mao, and G. E. Karniadakis, "DeepXDE: A deep learning library for solving differential equations," *SIAM Rev.*, vol. 63, no. 1, pp. 208–228, Jan. 2021, doi: 10.1137/19m1274067.

[57] E. Kharazmi, Z. Zhang, and G. E. Karniadakis, "Variational physics-informed neural networks for solving partial differential equations," 2019, *arXiv:1912.00873*.

[58] E. Kharazmi, Z. Zhang, and G. E. M. Karniadakis, "*hp*-VPINNs: Variational physics-informed neural networks with domain decomposition," *Comput. Methods Appl. Mech. Eng.*, vol. 374, Feb. 2021, Art. no. 113547, doi: 10.1016/j.cma.2020.113547.

[59] L. Yang, X. Meng, and G. E. Karniadakis, "B-PINNs: Bayesian physics-informed neural networks for forward and inverse PDE problems with noisy data," *J. Comput. Phys.*, vol. 425, Jan. 2021, Art. no. 109913, doi: 10.1016/j.jcp.2020.109913.

[60] K. Sun and X. Feng, "A second-order network structure based on gradient-enhanced physics-informed neural networks for solving parabolic partial differential equations," *Entropy*, vol. 25, no. 4, p. 674, Apr. 2023, doi: 10.3390/e25040674.

[61] D. M. Roh, M. He, Z. Bai, P. Sandhu, F. Chung, Z. Ding, S. Qi, Y. Zhou, R. Hoang, P. Namadi, B. Tom, and J. Anderson, "Physics-informed neural networks-based salinity modeling in the Sacramento–San Joaquin Delta of California," *Water*, vol. 15, no. 13, p. 2320, Jun. 2023, doi: 10.3390/w15132320.

[62] S. Singh, Y. E. Ebongue, S. Rezaei, and K. P. Birke, "Hybrid modeling of lithium-ion battery: Physics-informed neural network for battery state estimation," *Batteries*, vol. 9, no. 6, p. 301, May 2023, doi: 10.3390/batteries9060301.

[63] M. Zhou, G. Mei, and N. Xu, "Enhancing computational accuracy in surrogate modeling for elastic–plastic problems by coupling S-FEM and physics-informed deep learning," *Mathematics*, vol. 11, no. 9, p. 2016, Apr. 2023, doi: 10.3390/math11092016.

[64] M. Barreau, M. Aguiar, J. Liu, and K. H. Johansson, "Physics-informed learning for identification and state reconstruction of traffic density," in *Proc. 60th IEEE Conf. Decis. Control (CDC)*, Austin, TX, USA, Dec. 2021, pp. 2653–2658, doi: 10.1109/CDC45484.2021.9683295.

[65] Z. Mo, R. Shi, and X. Di, "A physics-informed deep learning paradigm for car-following models," *Transp. Res. C, Emerg. Technol.*, vol. 130, Sep. 2021, Art. no. 103240, doi: 10.1016/j.trc.2021.103240.

[66] R. Shi, Z. Mo, and X. Di, "Physics-informed deep learning for traffic state estimation: A hybrid paradigm informed by second-order traffic model," in *Proc. 35th AAAI Conf. Artif. Intell.*, 2021, pp. 540–547, doi: 10.1609/aaai.v35i1.16132.

[67] R. Shi, Z. Mo, K. Huang, X. Di, and Q. Du, "Physics-informed deep learning for traffic state estimation," 2021, *arXiv:2101.06580*.

[68] R. Shi, Z. Mo, K. Huang, X. Di, and Q. Du, "A physics-informed deep learning paradigm for traffic state and fundamental diagram estimation," *IEEE Trans. Intell. Transp. Syst.*, vol. 23, no. 8, pp. 11688–11698, Aug. 2022, doi: 10.1109/TITS.2021.3106259.

[69] E. Abreu and J. B. Florindo, "A study on a feedforward neural network to solve partial differential equations in hyperbolic-transport problems," in *Proc. Int. Conf. Comput. Sci. (ICCS)*, Krakow, Poland, 2021, pp. 398–411, doi: 10.1007/978-3-030-77964-1_31.

[70] M. J. Lighthill and G. B. Whitham, "On kinematic waves II. A theory of traffic flow on long crowded roads," *Proc. Roy. Soc. A, Math., Phys. Eng. Sci.*, vol. 229, no. 1178, pp. 317–345, 1955, doi: 10.1098/rspa.1955.0089.

[71] L. A. Pipes, "Vehicle accelerations in the hydrodynamic theory of traffic flow," *Transp. Res.*, vol. 3, no. 2, pp. 229–234, Jul. 1969, doi: 10.1016/0041-1647(69)90154-3.

[72] H. J. Payne, "Models of freeway traffic and control," in *Mathematical Models of Public Systems*. La Jolla, SC, USA: Simul. Councils, Inc., 1971, pp. 51–61.

[73] G. B. Whitham, *Linear and Nonlinear Waves*. New York, NY, USA: Wiley, 1974, pp. 1–636.

[74] W. Phillips, "A new continuum traffic model obtained from kinetic theory," in *Proc. IEEE Conf. Decis. Control Including 17th Symp. Adapt. Processes*, San Diego, NJ, USA, Jan. 1978, pp. 1032–1036, doi: 10.1109/CDC.1978.268087.

[75] Z. Wu, "Traffic flow dynamic modelling," *J. Fudan Univ., Natural Sci.*, vol. 30, no. 1, pp. 111–117, 1991, doi: 10.15943/j.cnki.fdxb-jns.1991.01.018.

[76] S. P. Hoogendoorn and P. H. L. Bovy, "Continuum modeling of multiclass traffic flow," *Transp. Res. B, Methodol.*, vol. 34, no. 2, pp. 123–146, Feb. 2000, doi: 10.1016/s0191-2615(99)00017-x.

[77] D. Helbing, A. Hennecke, V. Shvetsov, and M. Treiber, "MASTER: Macroscopic traffic simulation based on a gas-kinetic, non-local traffic model," *Transp. Res. B, Methodol.*, vol. 35, no. 2, pp. 183–211, Feb. 2001, doi: 10.1016/s0191-2615(99)00047-8.

[78] S. Cheng, L. Li, Y.-G. Liu, W.-B. Li, and H.-Q. Guo, "Virtual fluid-flow-model-based lane-keeping integrated with collision avoidance control system design for autonomous vehicles," *IEEE Trans. Intell. Transp. Syst.*, vol. 22, no. 10, pp. 6232–6241, Oct. 2021, doi: 10.1109/TITS.2020.2990211.

[79] W. Xu, and L. Xiong, "A study of the kinetic model congruent with car-following theory in one-dimensional traffic flow," *J. Transp. Syst. Eng. Inf. Technol.*, vol. 2, no. 1, pp. 42–44, 2002, doi: 10.3969/j.issn.1009-6744.2002.01.009.

[80] O. A. Ladyzhenskaya, "New equation for the description of the viscous incompressible fluids and solvability in the large of the boundary value problems for them," *Boundary value Problems Math. Phys.*, vol. 102, pp. 85–104, Jan. 1967.

[81] H. Yuan and Z. Yang, "A class of compressible non-newtonian fluids with external force and vacuum under no compatibility conditions," *Boundary Value Problems*, vol. 2016, no. 1, Dec. 2016, Art. no. 201, doi: 10.1186/s13661-016-0708-2.

[82] R. A. DeVore, R. Howard, and C. Micchelli, "Optimal nonlinear approximation," *Manuscripta Mathematica*, vol. 63, no. 4, pp. 469–478, Dec. 1989, doi: 10.1007/bf01171759.

[83] S. Liang and R. Srikant, "Why deep neural networks for function approximation?" 2016, *arXiv:1610.04161*.

[84] D. Yarotsky, "Error bounds for approximations with deep ReLU networks," *Neural Netw.*, vol. 94, pp. 103–114, Oct. 2017, doi: 10.1016/j.neunet.2017.07.002.

[85] K. He, X. Zhang, S. Ren, and J. Sun, "Delving deep into rectifiers: Surpassing human-level performance on ImageNet classification," in *Proc. IEEE Int. Conf. Comput. Vis. (ICCV)*, Santiago, Chile, Dec. 2015, pp. 1026–1034, doi: 10.1109/ICCV.2015.123.

[86] D.-A. Clevert, T. Unterthiner, and S. Hochreiter, "Fast and accurate deep network learning by exponential linear units (ELUs)," 2015, *arXiv:1511.07289*.

[87] A. L. Mass, A. Y. Hannun, and A. Y. Ng, "Rectifier nonlinearities improve neural network acoustic models," in *Proc. 30th Int. Conf. Mach. Learn. (ICML)*, Atlanta, GA, USA, 2013, pp. 3–9.

[88] G. Klambauer, T. Unterthiner, A. Mayr, and S. Hochreiter, "Self-normalizing neural networks," in *Proc. 31st Int. Conf. Neural Inf. Process. Syst. (NIPS)*, Long Beach, CA, USA, 2017, pp. 972–981.

[89] N. Boullé, Y. Nakatsukasa, and A. Townsend, "Rational neural networks," 2020, *arXiv:2004.01902*.

[90] A. Molina, P. Schramowski, and K. Kersting, "Padé activation units: End-to-end learning of flexible activation functions in deep networks," 2019, *arXiv:1907.06732*.

[91] Z. Chen, F. Chen, R. Lai, X. Zhang, and C.-T. Lu, "Rational neural networks for approximating graph convolution operator on jump discontinuities," in *Proc. IEEE Int. Conf. Data Mining (ICDM)*, Singapore, Nov. 2018, pp. 59–68, doi: 10.1109/ICDM.2018.00021.

[92] Y. Nesterov, "A method for unconstrained convex minimization problem with the rate of convergence $O(1/k^2)$," *Sov. Math. Doklady*, vol. 269, pp. 543–547, Jan. 1983.

[93] Y. Nesterov, "On an approach to the construction of optimal methods of minimization of smooth convex functions," *Matematicheskie Metody Resheniya Ekonomicheskikh Zadach*, vol. 24, pp. 509–517, Jan. 1988.

[94] Y. Nesterov, "Smooth minimization of non-smooth functions," *Math. Program.*, vol. 103, no. 1, pp. 127–152, May 2005, doi: 10.1007/s10107-004-0552-5.

[95] Y. Nesterov, "Gradient methods for minimizing composite functions," *Math. Program.*, vol. 140, no. 1, pp. 125–161, Aug. 2013, doi: 10.1007/s10107-012-0629-5.

[96] Y. Carmon, J. C. Duchi, O. Hinder, and A. Sidford, "'Convex until proven guilty': Dimension-free acceleration of gradient descent on non-convex functions," in *Proc. 34th Int. Conf. Mach. Learn. (ICML)*, Sydney, NSW, Australia, 2017, pp. 654–663.

[97] S. Ghadimi and G. Lan, "Accelerated gradient methods for nonconvex nonlinear and stochastic programming," *Math. Program.*, vol. 156, pp. 59–99, 2016.

[98] H. Li and Z. Lin, "Accelerated proximal gradient methods for nonconvex programming," in *Proc. 28th Int. Conf. Neural Inf. Process. Syst. (NIPS)*, Montreal, QC, Canada, Dec. 2015, pp. 7–12.

[99] Y. Xu and W. Yin, "A globally convergent algorithm for nonconvex optimization based on block coordinate update," *J. Sci. Comput.*, vol. 72, no. 2, pp. 700–734, Aug. 2017, doi: 10.1007/s10915-017-0376-0.

[100] Y. Carmon, J. C. Duchi, O. Hinder, and A. Sidford, "Accelerated methods for NonConvex optimization," *SIAM J. Optim.*, vol. 28, no. 2, pp. 1751–1772, Jan. 2018, doi: 10.1137/17m1114296.

[101] N. Agarwal, Z. Allen-Zhu, B. Bullins, E. Hazan, and T. Ma, "Finding approximate local minima faster than gradient descent," in *Proc. 49th Annu. ACM SIGACT Symp. Theory Comput.*, Montreal, QC, Canada, Jun. 2017, pp. 1195–1199, doi: 10.1145/3055399.3055464.

[102] C. Jin, P. Netrapalli, and M. I. Jordan, "Accelerated gradient descent escapes saddle points faster than gradient descent," 2017, *arXiv:1711.10456*.

[103] B. T. Polyak, "Some methods of speeding up the convergence of iteration method," *USSR Comput. Math. Math. Phys.*, vol. 4, no. 5, 1-17, 1964, doi: 10.1016/0041-5553(64)90137-5.

[104] E. D. Dolan and J. J. Moré, "Benchmarking optimization software with performance profiles," *Math. Program.*, vol. 91, no. 2, pp. 201–213, Jan. 2002, doi: 10.1007/s101070100263.

[105] D. Li and D. Zhu, "An affine scaling interior trust-region method combining with line search filter technique for optimization subject to bounds on variables," *Numer. Algorithms*, vol. 77, no. 4, pp. 1159–1182, Apr. 2018, doi: 10.1007/s11075-017-0357-2.

ZAN YANG was born in Jilin City, Jilin Province, China, in 1984. He received the B.S. degree in information and computing science from Dalian Nationalities University, Dalian, Liaoning, China, in 2008, the M.S. degree in basic mathematics from Beihua University, Jilin, in 2014, and the Ph.D. degree in basic mathematics from Jilin University, Jilin, in 2017.

From 2008 to 2011, he was a Hardware Engineer with the Headquarter of Da Tang Telecom. From 2017 to 2022, he was a Lecturer and the Secretary of the General Communist Party Branch, Deputy of Science, Tongji Zhejiang College. Since 2022, he has been a Lecturer with the Public Teaching and Research Department, Huzhou College. He is the author of more than 80 articles. His research interests include algorithms on machine learning, reinforcement learning, and their applications.

Dr. Yang is a lifetime member of the Chinese Association for Artificial Intelligence (CAAI) and the Operations Research Society of China (ORSC).

DAN LI was born in Tonghua, Jilin, China, in 1988. She received the B.S. degree in mathematics and applied mathematics and the M.S. degree in basic mathematics from Beihua University, Jilin, in 2011 and 2014, respectively, and the Ph.D. degree in operational research and cybernetics from Shanghai Normal University, Shanghai, China, in 2017.

From 2017 to 2022, she was a Lecturer with the Deputy of Science, Tongji Zhejiang College. Since 2022, she has been a Lecturer with the Public Teaching and Research Department, Huzhou College. She is the author of more than 30 articles. Her research interests include artificial intelligence related methodologies and their applications and convex and non-convex optimization theories.

Dr. Li is a lifetime member of the Chinese Association for Artificial Intelligence (CAAI) and the Operations Research Society of China (ORSC). She is one of the ''Leading Talents of Colleges and Universities (The Youth Talents)'' in Zhejiang province.

WEI NAI (Member, IEEE) was born in Nanjing, Jiangsu, China, in 1985. He received the B.S. degree in optical information science and technology and the M.S. degree in electromagnetic and microwave technology from the Beijing University of Posts and Telecommunications (BUPT), Beijing, China, in 2007 and 2010, respectively, and the Ph.D. degree in transportation information engineering and control from Tongji University, Shanghai, China, in 2013.

From 2014 to 2016, he was a Postdoctoral Researcher with the Postdoctoral Research Station of Control Science and Engineering, Tongji University. From 2017 to 2022, he was a Lecturer, an Associated Professor, the Principal of Sino-German exchanges, and the Vice Dean with the Department of Electronic and Information Engineering, Tongji Zhejiang College. Since 2022, he has been an Associate Professor with the School of Electronic Information, Huzhou College. He is the author of one book and over 130 articles. His current research interests include applied broadband communication and transportation behavior in information environment based on artificial intelligence algorithms.

Dr. Nai is a lifetime member of the Chinese Association for Artificial Intelligence (CAAI). He is one of the ''Leading Talents of Colleges and Universities (The Youth Talents)'' in Zhejiang Province, one of the first batch of ''Top-Notch Youth Talents in Education,'' one of the ''Outstanding Talents,'' one of the ''Excellent Teachers,'' and one of the first batch of ''Innovation and Entrepreneurship Advisors'' in the city of Jiaxing.

LU LIU was born in Tieling, Liaoning, China, in 1988. He received the B.S. and first M.S. degrees in transportation engineering from Tongji University, Shanghai, China, in 2009 and 2012, respectively, the second M.S. degree in transportation engineering from Oregon State University, USA, in 2014, and the Ph.D. degree in marketing from Syracuse University, USA, in 2020.

From 2019 to 2020, he was a Visiting Assistant Professor with Saginaw Valley State University. Since 2021, he has been an Assistant Professor of marketing with St. Bonaventure University. He is the author of ten articles. His research interests include statistical modeling, public policy, healthcare, and econometrics.

Dr. Liu is a member of the American Marketing Association (AMA).

JINGJING SUN was born in Zhoukou, Henan, China, in 1994. She received the B.S. degree in communication engineering from the Ocean University of China, Qingdao, Shandong, China, in 2015, and the M.S. degree in communication and information system from the University of Electronic Science and Technology of China, Chengdu, Sichuan, China, in 2018.

From 2018 to 2020, she was a Communication Algorithm Engineer with Hangzhou Guoxin Technology Company Ltd. Since 2020, she has been an Assistant Lecturer with the School of Electronic Information, Huzhou College. She is the author of four articles and three invention patents. Her research interests include wireless communication and artificial intelligence algorithms.

XIAOWEI LV was born in Lvliang, Shandong, China, in 1993. He received the B.S. degree in communication engineering and the M.S. degree in communication and information system from the University of Electronic Science and Technology of China, Chengdu, Sichuan, China, in 2015 and 2018, respectively.

From 2018 to 2020, he was a Communication Algorithm Engineer with Hangzhou Hikvision Digital Technology Company Ltd. Since 2020, he has been an Assistant Lecturer with the School of Electronic Information, Huzhou College. His research interests include embedded development and RF communication.